J. Fluid Mech. (2012), *vol.* 711, *pp.* 364–393. © Cambridge University Press 2012
doi:10.1017/jfm.2012.396

On non-self-similar regimes in homogeneous isotropic turbulence decay

Marcello Meldi† and Pierre Sagaut

Institut Jean Le Rond d'Alembert, UMR 7190, 4 Place Jussieu, Case 162, Université Pierre et Marie Curie, Paris 6, F-75252 Paris CEDEX 5, France

(Received 17 January 2012; revised 25 July 2012; accepted 2 August 2012;
first published online 11 September 2012)

Both theoretical analysis and eddy-damped quasi-normal Markovian (EDQNM) simulations are carried out to investigate the different decay regimes of an initially non-self-similar isotropic turbulence. Breakdown of self-similarity is due to the consideration of a composite three-range energy spectrum, with two different slopes at scales larger than the integral length scale. It is shown that, depending on the initial conditions, the solution can bifurcate towards a true self-similar decay regime, or sustain a non-self-similar state over an arbitrarily long time. It is observed that these non-self-similar regimes cannot be detected, restricting the observation to time exponents of global quantities such as kinetic energy or dissipation. The actual reason is that the decay is controlled by large scales close to the energy spectrum peak. This theoretical prediction is assessed by a detailed analysis of triadic energy transfers, which show that the largest scales have a negligible impact on the total transfers. Therefore, it is concluded that details of the energy spectrum near the peak, which may be related to the turbulence production mechanisms, are important. Since these mechanisms are certainly not universal, this may at least partially explain the significant discrepancies that exist between experimental data and theoretical predictions. Another conclusion is that classical self-similarity theories, which connect the asymptotic behaviour of either the energy spectrum $E(k \to 0)$ or the velocity correlation function $f(r \to +\infty)$ and the turbulence decay exponent, are not particularly relevant when the large-scale spectrum shape exhibits more than one range.

Key words: homogeneous turbulence, isotropic turbulence, turbulence theory

1. Introduction

In this paper we investigate the growth and time evolution of self-similar regimes in free decay of incompressible homogeneous isotropic turbulence (HIT).

Since the seminal studies of Taylor (1935), a huge amount of work has been devoted to freely decaying HIT: see Batchelor (1953), Hinze (1975), Monin & Yaglom (1975), Davidson (2004), Lesieur (2008) and Sagaut & Cambon (2008) for an exhaustive review. Nevertheless, several open issues are debated by the scientific community, and complete agreement about the different aspects related to the time evolution of freely decaying turbulence has not yet been reached.

† Email address for correspondence: marcellomeldi@gmail.com

https://doi.org/10.1017/jfm.2012.396 Published online by Cambridge University Press

Most theoretical works deal with self-similar decay regimes, which are classically defined as regimes that can be described using a single length scale $l(t)$ and a single velocity scale $u(t)$. Using this assumption, the three-dimensional energy spectrum can be expressed as $E(k,t) = u^2(t)l(t)F(kl(t))$, where k and F denote the wavenumber and a dimensionless shape function, respectively. Equivalently, the two-point longitudinal velocity correlation can be expressed as $\langle u(x,t)\,u(x+r,t)\rangle = u^2(t)f(r/l(t))$, where f is the two-point longitudinal correlation function.

Theoretical analyses rely mainly on one of the three following approaches: dimensional analysis of either the von Kármán–Howarth equation for $f(r)$ in physical space or the Lin equation for $E(k)$ in spectral space (George 1992; George & Wang 2009); analysis of a closed set of equations for turbulent kinetic energy $u^2(t)$ and dissipation rate $\varepsilon(t)$ (Speziale & Bernard 1992; Mansour & Wray 1994; Huang & Leonard 1994; Ristorcelli 2003; Ristorcelli & Livescu 2004; Ristorcelli 2006); and the Comte-Bellot–Corrsin method (Comte-Bellot & Corrsin 1966; Lesieur & Schertzer 1978), based on the consideration of a simplified spectrum shape and dimensional analysis.

One of the main results of these works is prediction of the evolution laws of global quantities, including the turbulent kinetic energy $u^2(t)$, dissipation rate $\varepsilon(t)$ and velocity turbulent integral scale $l(t)$. Specific attention has been paid to the possible existence of invariants (Oberlack 2002; Davidson 2009, 2011; Llor 2011; Vassilicos 2011), which are global quantities that should remain time-independent during turbulence decay. Their existence can be tied to some general physical conservation principles, and the identification of these invariants is still a controversial issue. Almost all theoretical works converge on the conclusion that kinetic energy and other global quantities should exhibit a power-law behaviour, e.g. $u^2(t) \propto t^{-n_{u^2}}$, but some significant differences exist concerning the value of the decay exponents. The experimental realization of exponentially decaying isotropic turbulence using fractal grids is still a controversial issue, but it can be predicted by dimensional analysis of the von Kármán–Howarth and Lin equations, assuming that the Taylor microscale is time-independent (George & Wang 2009; Mazellier & Vassilicos 2010; Krogstad & Davidson 2011, 2012). Works based on a spectral space approach connect the decay exponent and the energy distribution at very large scales, i.e they express the decay exponent n_{u^2} as a function of the slope of the energy spectrum at very small wavenumber σ. Assuming that the spectrum $E(k,t)$ is non-singular at $k=0$, the coefficient σ is often interpreted as being the coefficient such that $E(k\to 0) \propto k^{\sigma}$. A debated issue is the definition of the possible values of σ, which can be tied to the asymptotic behaviour of the correlation function $f(r\to+\infty) \propto r^{-m}$. Exponents m and σ can be expressed as a function of each other, thanks to the kinematic reciprocal relations that exist between $E(k)$ and $f(r)$. The most studied values are $\sigma = 2$ and $\sigma = 4$, since they are related to general conservation principles and historically famous invariant quantities. The former is related to conservation of linear momentum and the Birkhoff–Saffman invariant $L = \int \langle \boldsymbol{u}(\boldsymbol{x})\cdot\boldsymbol{u}(\boldsymbol{x}+\boldsymbol{r})\rangle \,\mathrm{d}\boldsymbol{r} \propto u^2(t)l^3(t)$ (Saffman 1967), and is referred to as the Saffman turbulence. The latter is associated with the conservation of angular momentum and the Loitsyansky invariant $I = \int \boldsymbol{r}^2\langle \boldsymbol{u}(\boldsymbol{x})\cdot\boldsymbol{u}(\boldsymbol{x}+\boldsymbol{r})\rangle \,\mathrm{d}\boldsymbol{r} \propto u^2(t)l^5(t)$, and is referred to as Batchelor turbulence, in recognition of Batchelor's seminal works. Besides the question of the existence of these two turbulent regimes and their associated self-similar regimes (e.g. Krogstad & Davidson 2010), the question arises of the physical relevance for other values of σ. This issue arises from the fact that, still assuming the regularity of $E(k)$ at $k=0$, the following Taylor series expansion holds: $E(k\to 0) = (L/4\pi^2)k^2 + (I/24\pi^2)k^4 + \cdots$. Both physical and mathematical arguments

https://doi.org/10.1017/jfm.2012.396 Published online by Cambridge University Press

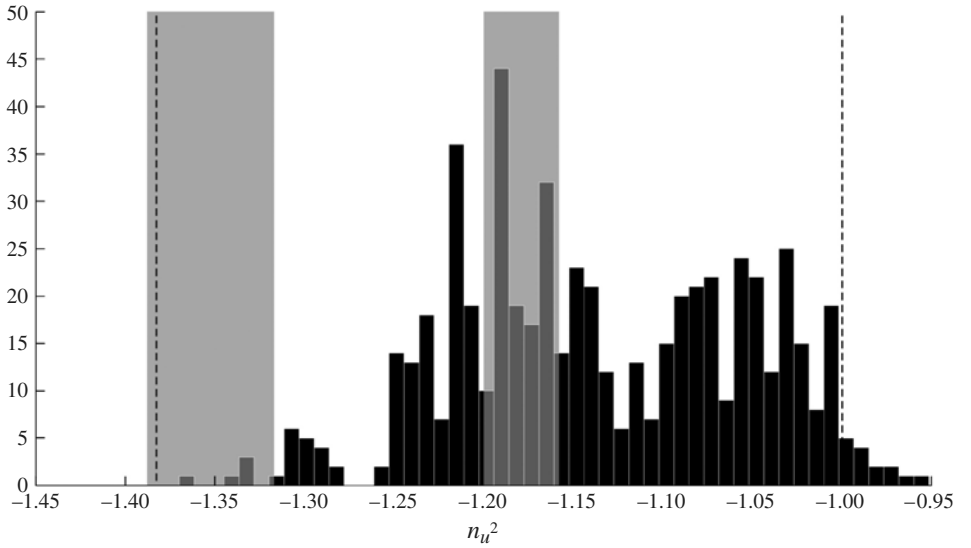

FIGURE 1. Histogram representing the distribution of the power-law exponent n_{u^2} related to the turbulent kinetic energy. The histogram is constructed from ∼650 experimental and direct numerical simulation (DNS) values published in international journals during the last 50 years. Shaded regions are related to possible values found by Meldi *et al.* (2011) via a generalized polynomial chaos-based uncertainty analysis for Saffman and Batchelor turbulence. Dashed vertical lines denote the minimum and maximum values given by uncertainty analysis considering a uniform distribution of σ within the interval $[1, 4]$.

lead to $1 \leqslant \sigma \leqslant 4$, but there is at present no general conclusion or consensus as to the occurrence of turbulent solutions with arbitrary real values of σ within the range $[1, 4]$. A very difficult point is that there is almost no direct experimental measure of σ: it is usually indirectly deduced from the measured power-law exponents of some global quantities by inverting an assumed relation between them. Another point is that direct numerical simulation with a good resolution of $E(k)$ at very large scales in the high Reynolds number regime is still beyond available supercomputer capabilities. Therefore, the main sources of realizations are still numerical simulations based on the closed Lin equation, in which the nonlinear transfer term is modelled by either local differential approximation models (e.g. Clark & Zemach 1998), or non-local closures such as the eddy-damped quasi-normal Markovian (EDQNM) model (e.g. Tchoufag, Sagaut & Cambon 2012).

An important point is that almost none of the theoretical predictions dealing with n_{u^2} have been clearly validated by experimental results up to now. To illustrate this point, the histogram of ∼650 values of n_{u^2} retrieved from experiments and direct numerical simulations published in international journals during the last 50 years is displayed in figure 1. The possible values associated with both $\sigma = 2$ and $\sigma = 4$ found in Meldi, Sagaut & Lucor (2011), considering realistic variations in the detailed shape of the energy spectrum, are also plotted. A striking observation is that most experimental data seem not to agree with theoretical results, showing that the fundamental issue of determining n_{u^2} is still open. Many interpretations of these discrepancies are possible, including the fact that turbulence decay may exhibit a marked sensitivity to initial conditions, which could differ from Saffman's and Batchelor's ideal cases (Valente & Vassilicos 2012).

https://doi.org/10.1017/jfm.2012.396 Published online by Cambridge University Press

The poor correlation between available data and theoretical results, on the one hand, and between different theories related to self-similar solutions, on the other hand, makes HIT decay one of the most important open fundamental issues in turbulence theory. To further investigate this issue, we choose here to address the question of the relation that may exist between the shape of the energy spectrum at very large scales and the power-law exponents of global physical quantities. To this end, non-self-similar solutions that depend on two independent length scales will be considered. It is important to emphasize that selecting self-similar solutions is an *a priori* choice, and that a few researchers have already considered non-self-similar solutions. Existence of self-similar solution is suggested by Lie-group symmetry analysis (Clark & Zemach 1998; Oberlack 2002) and observed in experimental results, direct numerical simulations and spectral-closure-based solutions (e.g. the EDQNM results in Lesieur 2008 and Sagaut & Cambon 2008), but no theoretical argument precludes the existence of other solutions that include more independent length scales. A cutoff length scale was introduced in Skrbek & Stalp (2000) at very small wavenumbers to account for saturation effects due to the finite size of physical realizations, while more general three-range composite energy spectra were briefly considered by Frenkel & Levich (1983), Frenkel (1984), Eyink & Thomson (2000) and Llor (2011). We present here a complete theoretical analysis of such three-range solutions, including possible breakdown of permanence of large eddies, and, for the first time, theoretical predictions are compared to numerical results. An EDQNM model is selected to obtain accurate investigation of very high Reynolds number cases with excellent spectral accuracy, for very long evolution times.

The paper is structured as follows. The EDQNM model is briefly discussed in § 2, a detailed discussion being available in the Appendix. The case of initial spectra with a single large-scale range is addressed § 3, in which theoretical results are compared with EDQNM simulations. Particular attention is paid to breakdown of permanence of large eddies in cases where distant triadic interactions become very strong at very large scales, and associated formulae for the time evolution exponents are proposed, extending previous results found in Eyink & Thomson (2000) and Lesieur (2008). The theoretical analysis of the three-range spectrum case is discussed in § 4, including corrections due to breakdown of permanence of large eddies. The theoretical predictions are then assessed via EDQNM results in § 5. Finally, conclusions are drawn in § 6.

2. The eddy-damped quasi-normal Markovian model

A brief description of the eddy-damped quasi-normal Markovian (EDQNM) model is given in this section. Details about the EDQNM model are given in the Appendix, and the reader is referred to Orszag (1970), Lesieur (2008) and Sagaut & Cambon (2008) for a more exhaustive discussion.

The EDQNM model is a quasi-normal closure used to predict triadic energy transfer. The model is derived under the assumption that the statistical moments of velocity components can be correctly represented closing the corresponding dynamic equations in wavenumber space. The closure is made by a model which takes into account the effects of fourth-order and higher moments by a linear eddy-damping on nonlinear energy transfer. This approximation prevents fast build-up of third-order moments, which can lead to non-physical solutions of the energy spectrum.

Numerical implementation of EDQNM relies on a logarithmic discretization in wavenumber space, and is able to predict accurately the three-point velocity

https://doi.org/10.1017/jfm.2012.396 Published online by Cambridge University Press

correlations between the elements of triads $[k, p, q]$. The wavenumber discretization is progressively less efficient when non-local very elongated triads $k \ll p \sim q$ are considered. This can have a significant impact on the accuracy of the predicted results, in particular if the two-point velocity correlation decays rapidly. Therefore, the original model proposed by Orszag is extended by adding a non-local transfer term which exactly estimates the distant non-local triadic interactions (Lesieur 2008).

The extended model, which has been assessed for both Saffman and Batchelor turbulence by comparison with the original model and theoretical results, exhibits significant improvement in the prediction of the slope of the energy spectrum in the case of Batchelor turbulence. In fact, a maximum error of less than 1 % is observed in the energy spectra obtained, while the original model yields errors of up to 8 %.

EDQNM makes it possible to get very accurate results at both very high and low Reynolds numbers, with good representation of both large and small scales. In the current simulations dealing with two-range initial energy spectra, more than 12 decades were simulated using 200 modes, while ∼17 decades have been considered for three-range spectrum cases with 290 modes. The large-scale part of the spectrum is very accurately represented in all cases: six decades for scales larger than the integral scale for two-range spectra at initial time, and nine decades for three-range spectra.

In all simulations, it was checked that at the final time the integral scale is at least 300 times larger than the first resolved mode and that $Re_\lambda \geqslant 170$, precluding possible corruption of the results by spurious saturation/confinement and low Reynolds number effects.

It is worth noting that such a resolution is far beyond the reach of direct numerical simulation or large eddy simulation, or most experimental set-ups for grid turbulence.

3. HIT decay imposing a single-range energy spectrum at large scales

According to classical self-similarity theories, it is possible to monitor the turbulent flow's decay regime by prescribing the longitudinal velocity correlation at large separation $u^2 f(r) \propto r^{-m}$, or equivalently the energy spectrum at very large scales $E(k \to 0) \propto k^\sigma$, where $\sigma = m - 1$ with $m < 5$. The invariant associated with the physical quantities u^2 and l, given by dimensional analysis, is $I_\sigma^{u^2 l} \propto u^2 l^{\sigma+1}$.

Robustness of the invariant obtained by EDQNM, along with accuracy in the prediction of the power-law coefficients related to the observed physical quantities, is now investigated. We will first restrict the analysis to initial energy spectra defined by a single range at large scales. In § 3.1, we will investigate the cases $\sigma = 1, 2, 3$: it is widely acknowledged that in these cases the 'permanence of large eddies' (PLE) hypothesis holds. We will then address the case of Batchelor turbulence in § 3.2, and finally extend the analysis to non-integer values $3 \leqslant \sigma \leqslant 4$.

All the results presented below are with reference to the normalized time $\tau = t/t_0$, with $t_0 = \varepsilon(0)^{-1/3} l(0)^{2/3}$ the characteristic turnover initial time.

3.1. EDQNM *simulations for* $\sigma = 1, 2, 3$

An energy spectrum with a single range at large scales for $\sigma = 1, 2, 3$ is first considered. A Comte-Bellot–Corrsin (CBC) energy spectrum (Comte-Bellot & Corrsin 1966) at $Re_\lambda = 10^4$ is imposed at initial time

$$E(k) = \begin{cases} A\, k^\sigma & kl \ll 1, \\ C_k\, \varepsilon^{2/3} k^{-5/3} & kl \gg 1, \end{cases} \tag{3.1}$$

https://doi.org/10.1017/jfm.2012.396 Published online by Cambridge University Press

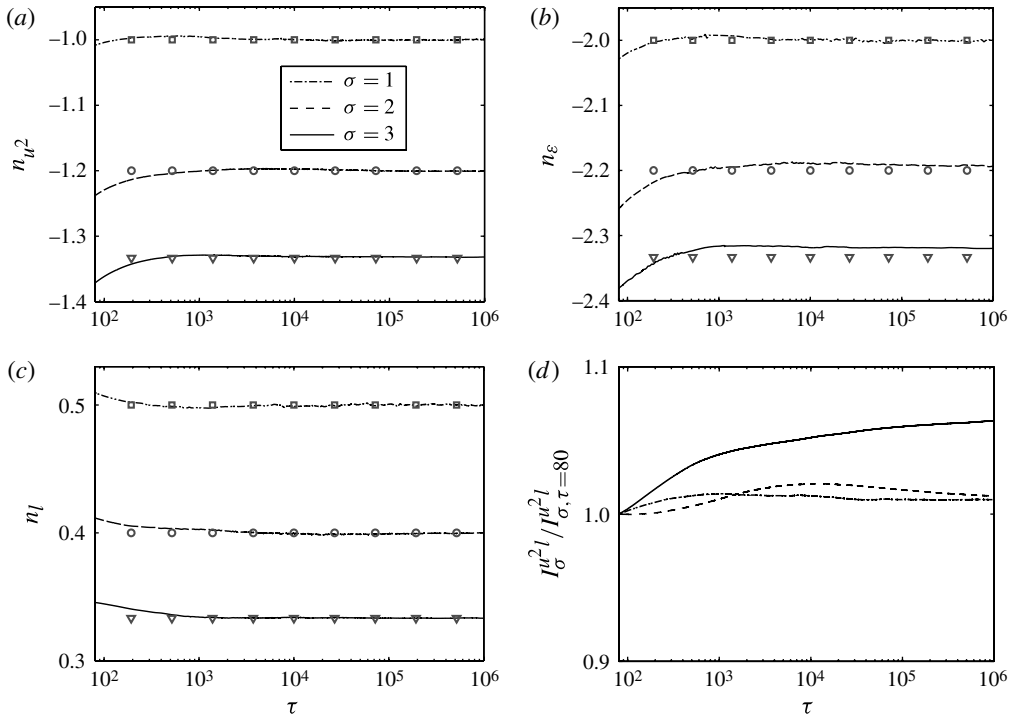

FIGURE 2. (*a–c*) Time evolution of power-law exponents and (*d*) the invariant based on the turbulent kinetic energy u^2 and the characteristic length l computed with an EDQNM code. The initial energy spectrum is imposed with a CBC functional form at $Re_\lambda = 10^4$ for $\sigma = 1, 2, 3$. Symbols are related to the CBC theoretical values.

where A and C_k are a σ-dependent coefficient and the Kolmogorov constant, respectively. The EDQNM simulations were carried out using a high resolution discretization for significantly long times. The very high Reynolds number imposed as an initial condition allows for the observation of the decay regime for a very long time before the effects of viscosity become relevant. In fact, the conditions $Re_\lambda > 200$ and $k_l = 1/l > 300\,k_0$ are satisfied at each time step, k_0 being the physical resolution of the numerical simulation. In all three cases, the invariance of the coefficient A is observed. This is a confirmation that the PLE hypothesis holds in these cases.

The computed power-law coefficients, as well as the invariant $I_\sigma^{u^2 l}$, are reported in figure 2. The reader may observe that the results are in very good agreement with the theoretical analysis by Comte-Bellot & Corrsin (1966). In fact, a maximum error of $\sim 0.5\,\%$ is observed in the prediction of the power-law coefficient of the dissipation rate ε for $\sigma = 3$. The reader should observe carefully that the results converge to the theoretical values after a long transient regime of the order of $10^4 t_0$. This transient regime is significant if compared to the simulated times in the direct numerical simulations reported in the literature; even though this result is obtained using EDQNM and does not necessarily comply with other numerical approaches, in particular with DNS, the discrepancies observed in numerical simulations when estimating power-law exponents may be partially due to low initial Reynolds numbers, for which viscosity effects become dominant before the transitory state has completely vanished.

https://doi.org/10.1017/jfm.2012.396 Published online by Cambridge University Press

The long time evolution of the invariant $I_\sigma^{u^2 l}$ is presented in figure 2(*d*). For all the values of σ, the invariant is found to be very stable over a very long time evolution. The time evolution of the normalized turbulent energy dissipation rate $C_\varepsilon = \varepsilon l / (u^2)^{3/2}$ has also been analysed. This parameter, which is null for each value of σ if computed by the CBC formula, has been observed to be a small positive quantity in grid turbulence due to spectral imbalance effects induced by turbulence decay: see Bos, Shao & Bertoglio (2007). Davidson (2011) estimates $C_\varepsilon(t) \propto t^{-p_0}, p_0 = 0.075$ and observes mild sensitivity of the parameter on the Reynolds number. In the present simulations, p_0 is observed to be a very small positive parameter, with a maximum value of $p_0 = 0.03$ for $\sigma = 3$.

The reported analysis confirms that the EDQNM code accurately obtains the power-law exponents and the invariants associated with the physical quantities. In particular, the invariant based on u^2 and l was observed to be exact even after a very long time evolution.

3.2. *Classical Batchelor turbulence case,* $\sigma = 4$

Batchelor turbulence is now investigated. This case is very popular because of the controversy concerning time-invariance of the Loitsyansky integral I. Within this framework, the longitudinal velocity correlation at large separation behaves as $u^2 f(r \to +\infty) \propto a_6 r^{-6}$. This corresponds to $E(k \to 0) = Ak^4$, with $A = I/24\pi^2$. In Davidson (2009), a theoretical framework is proposed to assess the conservation of the Loitsyansky integral in Batchelor turbulence. Results from several numerical simulations indicate that the coefficient a_6, and so I, exhibits weak time-dependence. Ishida, Davidson & Kaneda (2006) showed that, in direct numerical simulations at moderate Re_λ, a variation of $\approx 1\,\%$ is observed every 50 characteristic turnover times. These observations highlight the fact that the fast-decaying long-range velocity correlations associated with Batchelor turbulence are not consistent with the PLE hypothesis. Moreover, no experiments or simulations reported in the literature have ever found a power-law coefficient significantly close to the CBC formula in the case of Batchelor turbulence. In the comprehensive work by Mohamed & LaRue (1990), the lower observed value for the turbulent kinetic energy power-law coefficient is $n_{u^2} = -1.384$, which is significantly far from the value $n_{u^2} = -10/7$ obtained via the CBC formula. Eyink & Thomson (2000) argue that a loss of self-similarity of HIT decay can be the cause of the lack of agreement between numerical simulations and theoretical analysis. Considering the Loitsyansky integral as a time-dependent quantity, the following results are obtained (see Lesieur 2008; Sagaut & Cambon 2008):

$$A(t) \propto l^p(t), \tag{3.2}$$

$$l(t) \propto (t - t_0)^{2/(\sigma - p + 3)}, \tag{3.3}$$

$$u^2(t) \propto (t - t_0)^{2(\sigma - p + 1)/(\sigma - p + 3)}, \tag{3.4}$$

$$\varepsilon(t) \propto (t - t_0)^{-(3(\sigma - p) + 5)/(\sigma - p + 3)}, \tag{3.5}$$

where p is a correction term that can be numerically estimated. Eyink & Thomson (2000) estimate a value of $p = 0.55$.

In the analysis given below, we investigate the decay of Batchelor turbulence, observing the obtained power-law coefficient and invariants as in § 3.1. In this case, we impose initially a simplified version of the energy spectrum formulated

https://doi.org/10.1017/jfm.2012.396 Published online by Cambridge University Press

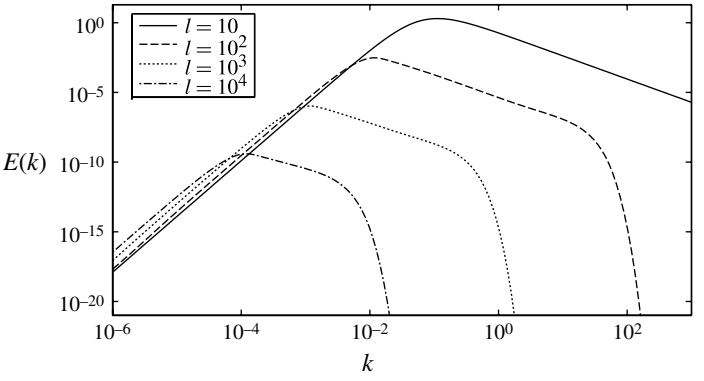

FIGURE 3. Time evolution of the energy spectrum obtained by EDQNM simulation in the case of Batchelor turbulence ($\sigma = 4$).

by Pope (2000):

$$E(k) = \begin{cases} A\,k^4 & kl \ll 1, \\ C_k\,\varepsilon^{2/3}k^{-5/3}f_l(kl) & kl \gg 1, \end{cases} \tag{3.6}$$

with

$$f_l(kl) = \left(\frac{kl}{[(kl)^\alpha + \beta]^{1/\alpha}}\right)^{5/3+\sigma}. \tag{3.7}$$

The free parameter α in (3.7) is set equal to 1.5, while the parameter β is computed in order to obtain $l(0) = 10$. This functional form of the energy spectrum is justified by the need to obtain an accurate estimate of the non-local energy transfer from the very first time steps. Indeed, an incorrect estimate of this energy transfer at the initial time, which is not negligible in the case of Batchelor turbulence, can lead to an error accumulation that does not disappear with the transitory time. The initial conditions $Re_\lambda(0) = 10^4$ and $\sigma = 4$ are imposed.

Figure 3 shows that the Loitsyansky integral in the formula $E(k) = I/(24\pi^2)k^4$ evolves over a very long time, as the energy spectrum is shifted in time. This is a clear signature of time-dependence of the coefficient A in (3.6). In the following, we will use the formula proposed by Eyink & Thomson (2000) and we will consider $A(t) \propto l^p(t)$. This formula has been observed to be very accurate in the case of Batchelor turbulence, as can be appreciated in figure 4(*a*). If the decay of the Re_λ is now considered, it is possible to observe in figure 4(*b*) that the decay process now almost agrees with the theoretical CBC formula for $\sigma = 4 - p, p = 0.52$. Conversely, the time evolution of Re_λ is far from the expected value obtained via the CBC formula for $\sigma = 4$. The results proposed by Eyink & Thomson (2000) are also consistent with the results obtained in the present work for the power-law coefficients of the physical quantities of interest, which are reported in figure 5(*a–c*). These conclusions are further supported by considering the invariant $I_4^{u^2 l}$: see figure 5(*d*). In fact, the invariant based on $\sigma = 4$ increases in time faster during the transitory state, but it is strongly time-dependent even after the transitory state has faded. Conversely, the invariant computed for $\sigma = 4 - p$ is almost constant after a transient time.

https://doi.org/10.1017/jfm.2012.396 Published online by Cambridge University Press

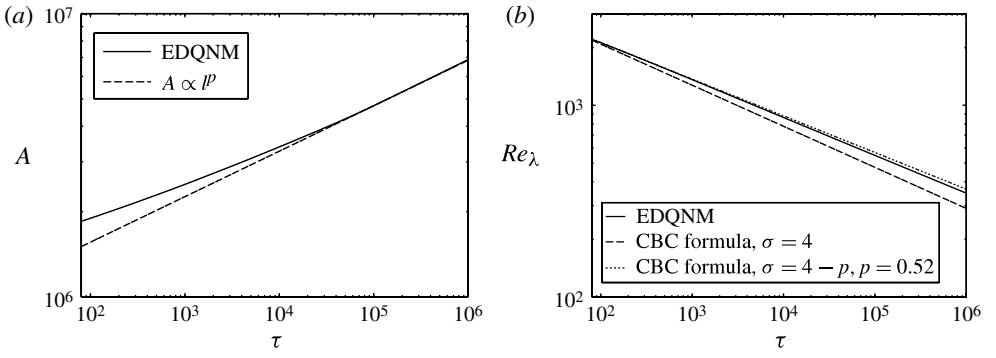

FIGURE 4. Time evolution of (*a*) the coefficient A at large scales, $E(k) = Ak^4$, and (*b*) the Re_λ number obtained by EDQNM simulation in the case of Batchelor turbulence ($\sigma = 4$).

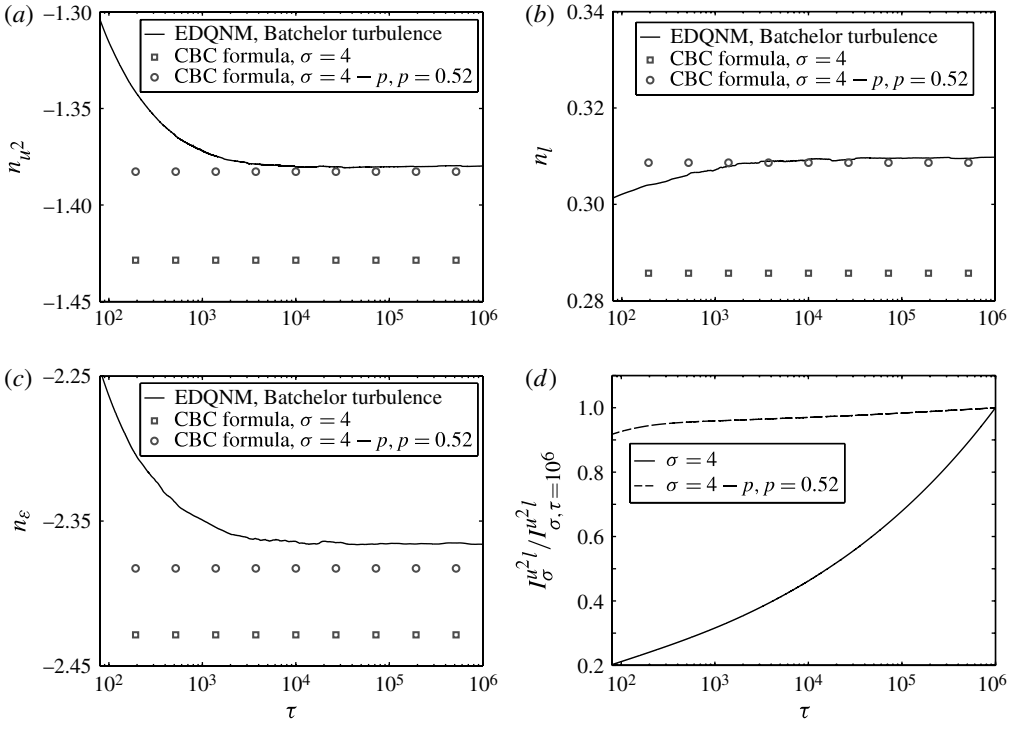

FIGURE 5. Time evolution of power-law exponents for (*a*) the turbulent kinetic energy u^2, (*b*) the characteristic length l, and (*c*) the dissipation rate ε. (*d*) The invariant based on u^2 and l, for two different values of the parameter σ. The initial energy spectrum is imposed following (3.6) at $Re_\lambda = 10^4$, for $\sigma = 4$. Symbols are related to the CBC theoretical values.

This behaviour can be related to non-local energy transfers. The backward energy cascade is more significant at very large scales for increasing σ. The inverse energy cascade is strong enough to alter the very large scales significantly, resulting in a shift of the energy spectrum associated with time-dependence of the Loitsyansky integral I. From another point of view, the contribution of non-local energy transfer may become

https://doi.org/10.1017/jfm.2012.396 Published online by Cambridge University Press

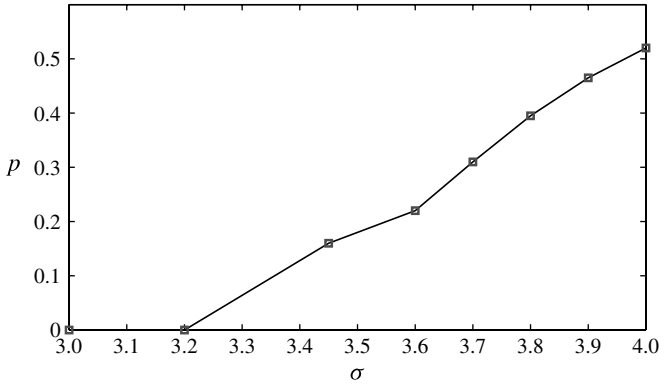

FIGURE 6. Dependence of the parameter p on the σ parameter imposed on the energy spectrum at the initial time. The parameter p was obtained from the computed power-law coefficient of the physical quantities analysed, inverting the CBC formula.

relevant when $u^2 f$ decays fast enough. The parameter p is actually a measure of the magnitude of the effects of non-local energy transfer.

Eyink & Thomson (2000) concluded that no self-similar decay can occur in the range $4 - p < \sigma < 4, p \approx 0.55$ while self-similar decay is present for $-1 < \sigma < 4 - p$ and so, for any σ initially imposed, $p = \sigma - 3.45, \sigma \geqslant 3.45$ and $p = 0, \sigma < 3.45$. We will show in the following that the results obtained by EDQNM simulation indicate that the dependence of $p(\sigma)$ is more complex, and that the value $\sigma = 4 - 0.55$ does not necessarily correspond to a self-similar regime.

To check the sensitivity of the parameter p versus σ, several EDQNM simulations have been performed in the range $3 \leqslant \sigma \leqslant 4$. For each simulation, the p exponent was deduced from the recovered power-law exponent by inverting the appropriate CBC formula. The results are reported in figure 6, where it is seen that the dependence of the parameter p on σ is approximately linear and can be expressed as $p = a(\sigma - n_0)$ for values of $\sigma > n_0 \approx 3.2$, a being a constant. The results show that $a \approx 0.65 < 1$, whereas Eyink & Thomson (2000) *a priori* assumed that $a = 1$. These results are in agreement with the probability density functions of the power-law exponents recovered by Meldi *et al.* (2011), which show significantly higher probability of obtaining n values in the range $3 \leqslant \sigma \leqslant 3.4$. The coefficient p also shows moderate dependence on the initial shape of the energy spectrum, supporting the conclusion that the parameter p represents a physical response of the turbulent flow to non-local energy transfers. This is the reason why, using a different initial energy spectrum, Eyink & Thomson (2000) recovered a value of $p \approx 0.55$, while in the present set of simulations $p = 0.52$ has been the value that best fits the data observed from power-law exponents and invariants.

3.3. *Analysis of the long-range velocity correlations $u^2 f$*

The analysis performed for the classical cases $\sigma = 1, 2, 3, 4$ is completed by a direct computation of the long-range velocity correlations $u^2 f$. Given the energy spectrum at a given time t, the correlation $u^2 f$ can be exactly recovered by the integral

$$u^2 f(r, t) = 2 \int_0^{+\infty} \mathrm{d}k E(k, t) \left(\frac{\sin(kr)}{k^3 r^3} - \frac{\cos(kr)}{k^2 r^2} \right). \tag{3.8}$$

https://doi.org/10.1017/jfm.2012.396 Published online by Cambridge University Press

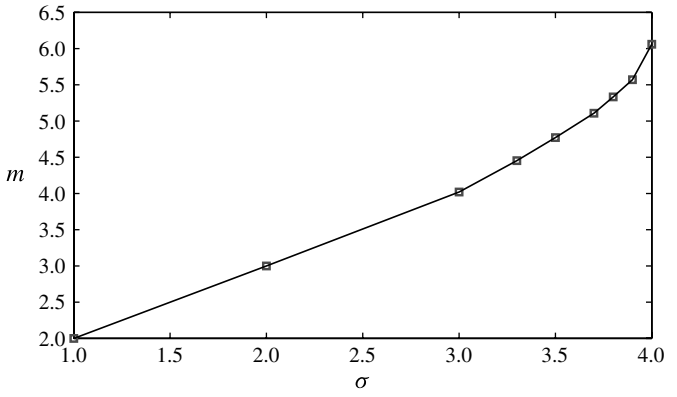

FIGURE 7. Dependence of the parameter m on the σ parameter imposed on a CBC energy spectrum. The parameter m was obtained by using (3.8).

Equation (3.8) is first used to estimate by linear regression the power-law coefficient m of the long-range velocity correlations starting from a CBC energy spectrum for $1 \leqslant \sigma \leqslant 4$. The results, which are shown in figure 7, are in agreement with the results discussed by Davidson (2011). The relation is then considered to investigate the energy spectra obtained by EDQNM. The spectra were sampled at time t satisfying the relation $l(t) = 200$. The choice was made to analyse the velocity correlations once the power-law coefficient of the physical quantities analysed reached convergence.

The results reported in figure 8 again exhibit excellent agreement with those discussed by Davidson (2011), the maximum value of the parameter r investigated being limited by the spectral resolution of the numerical simulations. The computed coefficient m is $m = 2, 3.01, 3.96, 6.14$ for $\sigma = 1, 2, 3, 4$, respectively. In particular, it is possible to appreciate that the long-range velocity correlation power-law coefficient $m = 6$ has been recovered in the case of Batchelor turbulence. This last point confirms that the differences arising when comparing the EDQNM simulation of Batchelor turbulence with a CBC formula do not stem from incorrect representation of the long-range velocity correlation, but are due to a non-negligible energy transfer contribution correlated to non-local triadic interactions.

4. Theoretical analysis for composite three-range spectra

In § 3, we analysed HIT decay via EDQNM and observed that the numerical results progressively deviate from the theoretical CBC formula at high σ values. We now propose a theoretical development starting from a composite three-range energy spectrum, in order to investigate the evolution of the decay regime when the characteristics of the energy spectrum at large scales are governed by several parameters. This composite energy spectrum is defined by the existence of two ranges at large scales. HIT decay starting from a composite three-range energy spectrum has already been addressed theoretically in Frenkel & Levich (1983), Frenkel (1984) and Llor (2011). The energy spectrum is thus described by three different regions, each defined by a different analytical expression: the very large-scale region, $0 \leqslant k \leqslant k_1$, in which the energy spectrum is given by $E(k) = Ak^{\sigma_1}$; the large-scale region, $k_1 \leqslant k \leqslant k_2$, characterized by a slope parameter σ_2; and the inertial region, $k \geqslant k_2$, in which the inertial range by Kolmogorov (1941) is observed. Here k_1 and k_2 are associated with

https://doi.org/10.1017/jfm.2012.396 Published online by Cambridge University Press

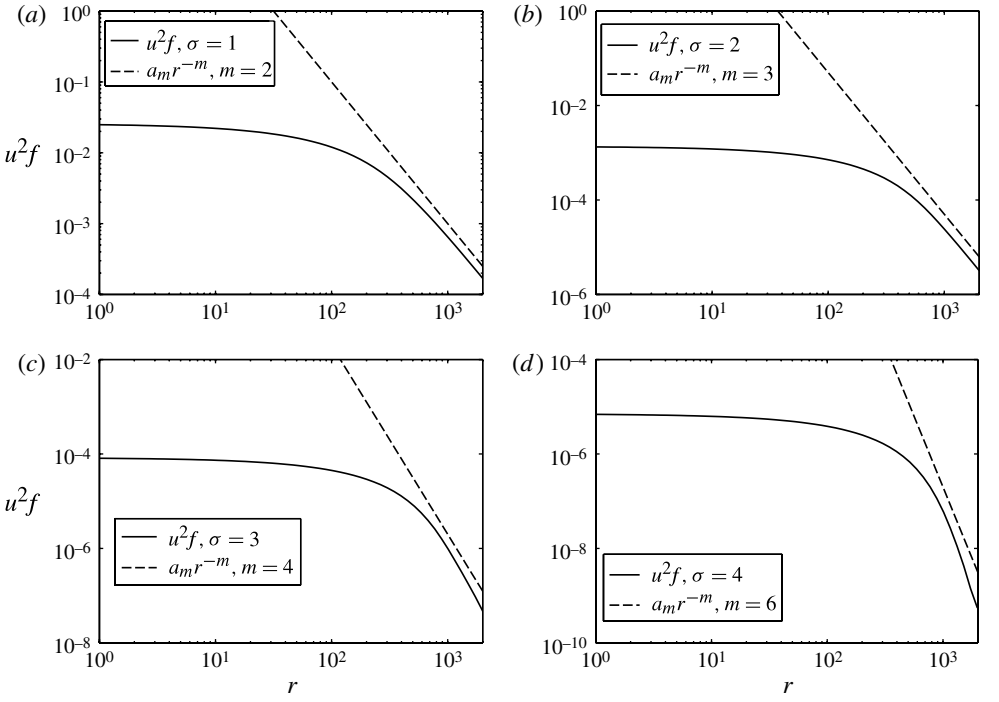

FIGURE 8. Long-range velocity correlations u^2f obtained by EDQNM simulations. A classical two-range energy spectrum for $\sigma = 1, 2, 3, 4$ at $Re_\lambda = 10^4$ is initially imposed; r is expressed in the characteristic length scale l units.

two independent length scales, $l_1 = 1/k_1$ and $l_2 = 1/k_2$. The reader should observe that the length l_2 is usually referred to as the characteristic length (l in the two-range cases discussed above) of the flow, as it is associated with the peak of the energy spectrum.

The full analytical functional form is

$$E(k) = \begin{cases} A\,k^{\sigma_1} & kl_1 \ll 1, \\ B\,k^{\sigma_2} & kl_1 \gg 1,\ kl_2 \ll 1, \\ C_k\varepsilon^{2/3}k^{-5/3} & kl_2 \gg 1. \end{cases} \tag{4.1}$$

This functional form is completed by the relations

$$A\,l_1^{-\sigma_1} = B\,l_1^{-\sigma_2} \quad \text{or} \quad A\,k_1^{\sigma_1} = B\,k_1^{\sigma_2}, \tag{4.2}$$

$$B\,l_2^{-\sigma_2} = C_k\varepsilon^{2/3}l_2^{5/3} \quad \text{or} \quad B\,k_2^{\sigma_2} = C_k\varepsilon^{2/3}k_2^{-5/3}, \tag{4.3}$$

which denote the continuity of the energy spectrum at $k_1 = 1/l_1$ and $k_2 = 1/l_2$. Let us now express the coefficients A and B using (3.2):

$$A(t) \propto l_1^{p_1}(t), \quad B(t) \propto l_2^{p_2}(t). \tag{4.4}$$

The coefficients p_1 and p_2 are equal to 0 if the PLE hypothesis holds. We recall that the formula used to describe the time evolution of the coefficients A and B is not an arbitrary model, chosen by the authors, but the result of the theoretical framework proposed by Eyink & Thomson (2000).

https://doi.org/10.1017/jfm.2012.396 Published online by Cambridge University Press

As mentioned in § 1, it is possible to obtain the decay law of the physical quantities related to the flow by dimensional analysis. A classical example was proposed by Kolmogorov (1941), who showed that by using dimensional analysis it is possible to express the decay of the turbulent kinetic energy u^2 as a function of the dissipation rate ε:

$$\frac{\partial u^2}{\partial t} \propto -\varepsilon. \tag{4.5}$$

The expressions of the physical quantities ε and u^2 can be linked if an analytical form of the energy spectrum is prescribed. Let us consider the value of u^2 at time t:

$$u^2(t) = \frac{1}{2}\int_0^{+\infty} E(k,t)\,\mathrm{d}k. \tag{4.6}$$

Integrating the energy spectrum illustrated in (4.1), we obtain

$$u^2 = \frac{1}{2}\left(\left[\frac{A}{\sigma_1+1}k^{\sigma_1+1}\right]_0^{1/l_1} + \left[\frac{B}{\sigma_2+1}k^{\sigma_2+1}\right]_{1/l_1}^{1/l_2} + \left[\frac{-3C_k}{2}\,\varepsilon^{2/3}\,k^{-2/3}\right]_{1/l_2}^{+\infty}\right). \tag{4.7}$$

Equation (4.7) can be conveniently rewritten as a sum of four terms:

$$u^2 = \frac{1}{2}\left(\frac{A}{\sigma_1+1}l_1^{-(\sigma_1+1)} + \frac{B}{\sigma_2+1}l_2^{-(\sigma_2+1)} - \frac{B}{\sigma_2+1}l_1^{-(\sigma_2+1)} + \frac{3C_k}{2}\,\varepsilon^{2/3}\,l_2^{2/3}\right). \tag{4.8}$$

It can be observed that the second and fourth terms of (4.8) are the terms obtained from the u^2 integration using a CBC functional form of the energy spectrum, while the first and third terms are due to the change of slope of the energy spectrum at k_1. Using the two continuity equations (4.2)–(4.3), it is possible to simplify (4.8) in order to define the turbulent kinetic energy u^2 as a function of the sole dissipation rate ε, leading to

$$u^2 = u^2(\varepsilon, \sigma_1, \sigma_2, A, B). \tag{4.9}$$

Let us consider the ideal case $l_1 \gg l_2$ and group the second and fourth terms and first and third terms of (4.8):

$$u^2 = \left(\frac{3\sigma_2+5}{4(\sigma_2+1)}C_k^{(3+3\sigma_2)/(5+3\sigma_2)}B^{2/(5+3\sigma_2)}\right)\varepsilon^{2(\sigma_2+1)/(5+3\sigma_2)} + \frac{\sigma_2-\sigma_1}{2(\sigma_1+1)(\sigma_2+1)}B^{2/3}\left(\frac{A}{B}\right)^{(\sigma_2+1)/(\sigma_2-\sigma_1)}. \tag{4.10}$$

The second term of the equation represents a variation of the total energy of the system, due to the different slope of the energy spectrum at very large scales. Let us define the *decaying energy* u_e^2 as

$$u_e^2 = u^2 - \frac{\sigma_2-\sigma_1}{2(\sigma_1+1)(\sigma_2+1)}B^{2/3}\left(\frac{A}{B}\right)^{(\sigma_2+1)/(\sigma_2-\sigma_1)}. \tag{4.11}$$

This new quantity is the energy that the system would have in the case of a CBC starting energy spectrum with a $\sigma_1 = \sigma_2$, and it obviously has a physical meaning only if two or more ranges are considered at large scales. The CBC theoretical analysis is exactly recovered if u_e^2 is considered in place of u^2. Furthermore, if $l_1 \gg l_2$, the effective energy u_e^2 tends to the limit of the turbulent kinetic energy u^2,

https://doi.org/10.1017/jfm.2012.396 Published online by Cambridge University Press

so the equality $u_e^2 = u^2$ is recovered. In fact, the continuity equations show that $(A/B)^{(\sigma_2+1)/(\sigma_2-\sigma_1)} = k_1^{\sigma_2+1} \approx l_1^{-(\sigma_2+1)}$ and $B^{2/3} \approx (E_{max}(0) l_2^{\sigma_2}(0))^{2/3}$. If $l_1 \gg l_2$, the second term of (4.10) tends to zero and $u_e^2 \to u^2$.

Substituting (4.11) in (4.10), one obtains

$$u_e^2 = D\, \varepsilon^{2(\sigma_2+1)/(5+3\sigma_2)}, \tag{4.12}$$

where D is a constant. The decay law depends only on σ_2. Evidently the shape of the energy spectrum at very large scales does not influence the decay law of the physical quantities of interest, but it is taken into account in the definition of the effective energy of the system. Combining (4.12) and (4.5), the following decay law can be obtained after integration:

$$u_e^2(t) = E\ (t - t_1)^{-2(\sigma_2+1)/(\sigma_2+3)}. \tag{4.13}$$

This is exactly the same as the formula derived by Comte-Bellot & Corrsin (1966) starting from a simpler functional form of the energy spectrum. Equivalently, the CBC formula can be derived for all the other physical quantities under consideration. An interesting point is the lack of evidence in the theoretical framework that these quantities have to be corrected in a similar way to turbulent kinetic energy. Equation (4.13) is compatible with the Kolmogorov decay law if $\sigma_2 = 4$; nevertheless, for $\sigma_2 > 3.2$, the effective value of σ_2 must be corrected by the term $p(\sigma_2)$ in order to take into account the effects of the non-local energy transfers. It is also worth noting that, although the spectrum exhibits two independent length scales at low wavenumber, the evolution of the system is similar to a classical self-similar solution. Therefore, such a state can be referred to as a pseudo-self-similar state.

In summary, it can be observed that the power-law coefficients associated with HIT decay are not sensitive to the characteristics of the energy spectrum at the largest scales. The shape of the energy spectrum close to the peak of energy seems to be of primary importance. The characteristics of the energy spectrum at the largest scales simply modify the definition of decaying energy u_e^2 of the system. These considerations are in agreement with the numerical results observed by Meldi *et al.* (2011), which discovered dependence of the power-law coefficients n_Q when considering uncertainties in the shape of the energy spectrum in the proximity of its peak.

The theoretical framework proposed in the present paper is valid for the early stages of HIT decay, which are represented in figure 9(*a*) and for which the relation $l_1 \gg l_2$ holds. The two length scales l_1 and l_2 evolve in time with different power laws, and they can possibly become identical at a critical time t_c. Finally a two-range energy spectrum will be observed, as in figure 9(*b*) for $t > t_c$, if the scale l_2 grows faster than l_1. From a direct application of the CBC formula, and taking into account the non-local correction term, we know that $l_2(t) \propto t^{2/(\sigma_2-p_2+3)}$. Let us now consider the time evolution of the length scale l_1. By manipulating the continuity equations (4.2)–(4.3), one obtains

$$l_1^{(\sigma_2-\sigma_1)} = \frac{B}{A}. \tag{4.14}$$

Substituting the coefficients A and B by power laws based on the associated characteristic length, the time-dependence of the scale l_1 can be expressed as

$$l_1 \propto t^{2p_2/(\sigma_2-\sigma_1+p_1)(\sigma_2-p_2+3)}. \tag{4.15}$$

https://doi.org/10.1017/jfm.2012.396 Published online by Cambridge University Press

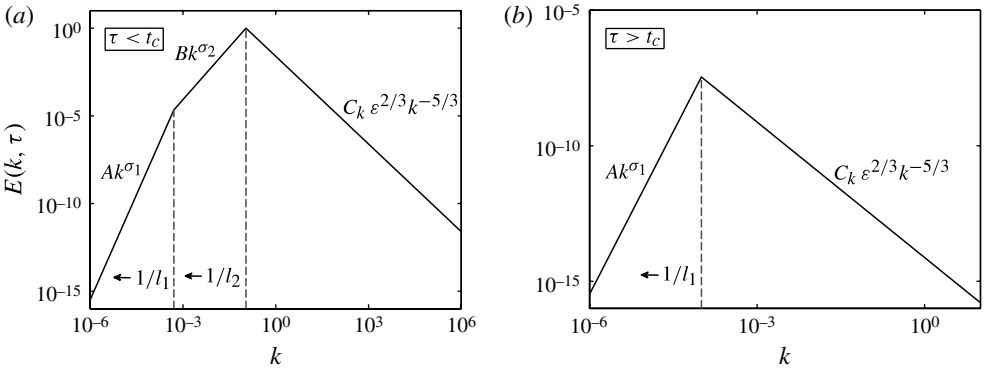

FIGURE 9. Scheme of the time evolution of the composite three-range energy spectrum (*a*) before and (*b*) after the critical time t_c.

Equation (4.15) shows that if the condition $p_2 = 0$ holds, the scale l_1 will be constant throughout the self-similar regime, while a time evolution will be observed for positive values of the parameter p_2. The critical time will still be a finite quantity if the scale l_2 grows faster in time than the scale l_1:

$$\frac{2p_2}{(\sigma_2 - \sigma_1 + p_1)(\sigma_2 - p_2 + 3)} < \frac{2}{(\sigma_2 - p_2 + 3)}. \tag{4.16}$$

In the case

$$\sigma_2 - \sigma_1 + p_1 < 0, \tag{4.17}$$

the scale l_1 will decrease in time, and the two length scales will collide after a finite decay time. Conversely, if $\sigma_2 - \sigma_1 + p_1 > 0$, a finite critical time will be recovered if $\sigma_1 - p_1 < \sigma_2 - p_2$. If $p_2 > 0$, the inequality is always satisfied for $\sigma_1 \leqslant 3.2$. We can then deduce that, if $p_1 = 0$ or $p_2 = 0$, the critical time will be finite. If both $p_1 > 0$ and $p_2 > 0$, the critical time can diverge to infinity, leading to a non-self-similar regime. The conditions

$$\begin{cases} \sigma_2 - \sigma_1 + p_1 > 0 \\ \sigma_1 - p_1 > \sigma_2 - p_2 \;\rightarrow\; \sigma_1 > \sigma_2 \end{cases} \tag{4.18}$$

will have to hold in order for an infinite critical time to be observed. The black region in figure 10 represents the value of the parameters $[\sigma_1, \sigma_2]$ for which $t_c = +\infty$. Combining (4.18), the evolution of a non-self-similar regime will be observed if $\sigma_1 - p_1 < \sigma_2 < \sigma_1$.

If the effects of the initial transient are neglected, an approximation to the critical time can easily be deduced from the power law describing the decay of the two scales. At time t_c the following relation is satisfied:

$$l_1(0)\, {t_c}^{2p_2/(\sigma_2-\sigma_1+p_1)(\sigma_2-p_2+3)} = l_2(0)\, {t_c}^{2/(\sigma_2-p_2+3)}. \tag{4.19}$$

Equation (4.19) can be manipulated to obtain the critical time t_c as

$$t_c = (l_2(0)/l_1(0))^{\alpha_c}, \quad \alpha_c = \frac{1}{2}\frac{(\sigma_2 - \sigma_1 + p_1)(\sigma_2 - p_2 + 3)}{(\sigma_1 - p_1) - (\sigma_2 - p_2)}. \tag{4.20}$$

https://doi.org/10.1017/jfm.2012.396 Published online by Cambridge University Press

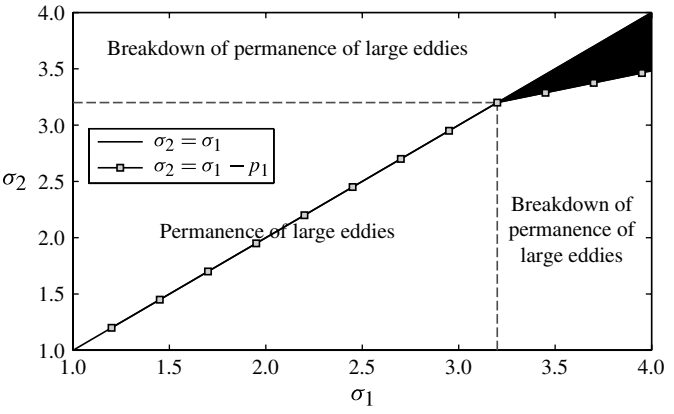

FIGURE 10. Values of the parameters σ_1, σ_2 leading to a finite critical time (white) and an infinite critical time (black).

	n_{u^2}	n_l	n_ε
$t < t_c$	$2(\sigma_2 - p_2 + 1)/(\sigma_2 - p_2 + 3)$	$2/(\sigma_2 - p_2 + 3)$	$(3(\sigma_2 - p_2) + 5)/(\sigma_2 - p_2 + 3)$
$t > t_c$	$2(\sigma_1 - p_1 + 1)/(\sigma_1 - p_1 + 3)$	$2/(\sigma_1 - p_1 + 3)$	$(3(\sigma_1 - p_1) + 5)/(\sigma_1 - p_1 + 3)$

TABLE 1. Analytical formulae obtained by the theoretical approach derived from the analysis of the three-range energy spectrum, in the case of a finite value of the critical time t_c.

An important deduction from the above analysis is that the three-range spectrum will undergo a transition to a two-range spectrum if one of the ranges is initially imposed with a slope coefficient σ for which the PLE hypothesis is satisfied.

At the critical time t_c, the second and third terms in (4.8) will cancel out, and the theoretical analysis will become identical to the two-range spectrum case discussed above. The parameter σ_1 will govern the decay regime and the characteristic velocity of the flow will be related to the turbulent kinetic energy u^2. The results of the analysis are summarized in table 1, which shows a transition between a pseudo-self-similar and a true self-similar regime, whose characteristics are driven by the parameters σ_2 and σ_1, respectively. In particular, an invariant based on σ_2 will no longer be invariant after the bifurcation of the decay regime. Conversely, some time-evolving quantities considered will become invariants as the turbulent flow turns out to be sensitive to the parameter σ_1. The transition between the two states will be smooth, since when l_1 and l_2 are sufficiently close, scales belonging to both ranges are involved in the energy cascade process. In particular, it is not possible to deduce the time evolution of the shape of the energy spectrum between the two length scales $l_1(t)$ and $l_2(t)$ from the theoretical framework proposed. In § 5, this point will be investigated by using EDQNM simulations.

5. EDQNM results for composite three-range energy spectra

The theoretical analysis reported in § 4 will now be assessed by comparison with EDQNM results, imposing a composite three-range initial energy spectrum

https://doi.org/10.1017/jfm.2012.396 Published online by Cambridge University Press

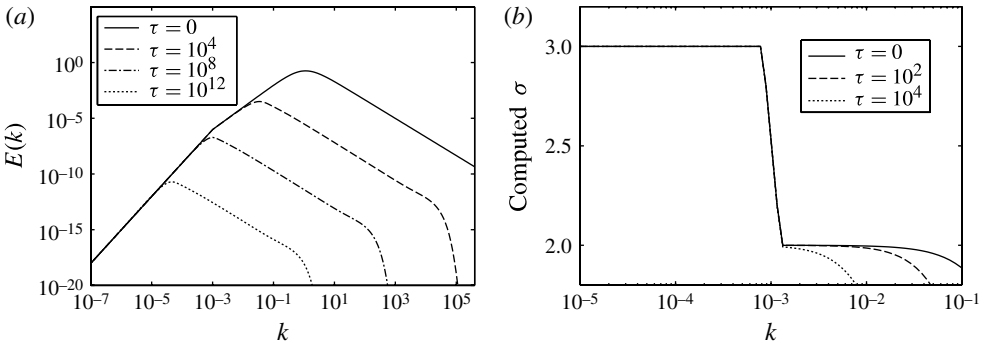

FIGURE 11. (*a*) Time-evolving energy spectra and (*b*) corresponding slope for a composite three-range initial energy spectrum. The case of $\sigma_1 = 3$ and $\sigma_2 = 2$ is investigated.

at $Re_\lambda(0) = 10^5$. The initial energy spectrum is inspired by Pope's model spectrum (see Pope 2000):

$$E(k) = \begin{cases} A\,k^{\sigma_1} & kl_1 \ll 1, \\ C_k\,\varepsilon^{2/3}k^{-5/3}f_l(kl_2) & kl_1 \gg 1, \end{cases} \tag{5.1}$$

with

$$f_l(kl_2) = \left(\frac{kl_2}{[(kl_2)^\alpha + \beta]^{1/\alpha}}\right)^{5/3+\sigma_2}. \tag{5.2}$$

This formulation smoothly connects the second range at large scales with the Kolmogorov inertial range. The smoothness of this transition is controlled by the parameter α, which is set to $\alpha = 1.5$ as in the study of Batchelor turbulence reported in § 3.2. In the same way, the parameter β is fixed to impose the condition $l_2(0) = 1$ for all initial conditions considered. The length scales l_1 and l_2 are initially separated by three decades, i.e. $l_1 = 10^3\,l_2$. The corresponding condition $l_0 = 10^6 l_1$ is initially imposed.

First, cases in which the PLE hypothesis holds are considered in § 5.1. In these cases, there is finite critical time. Decay with finite critical time but with PLE breakdown is investigated in § 5.2. Finally, cases with infinite critical time t_c, i.e. cases in which the flow never reaches a true self-similar state, are considered in § 5.3.

5.1. *Three-range energy spectrum with PLE hypothesis satisfied*

We now consider σ values for which the PLE hypothesis is satisfied. The case of $\sigma_1 = 3$ and $\sigma_2 = 2$ is selected. Using (4.20), we can expect the transition between the two regimes to occur at a critical time $t_c = 10^{7.5}t_0$.

The numerical results are in excellent agreement with the theoretical framework proposed. As seen in figure 11, which displays the energy spectrum and its slope, the length scale l_1 does not vary in time as the turbulent flow decays and the three-range-shape of the energy spectrum is conserved until the length scale l_2 reaches the same order of magnitude as the scale l_1. The transition is smooth, as observed in figure 12, where the time evolution of Re_λ is plotted. The largest scales are frozen in this case, since they do not evolve until the critical time is reached.

https://doi.org/10.1017/jfm.2012.396 Published online by Cambridge University Press

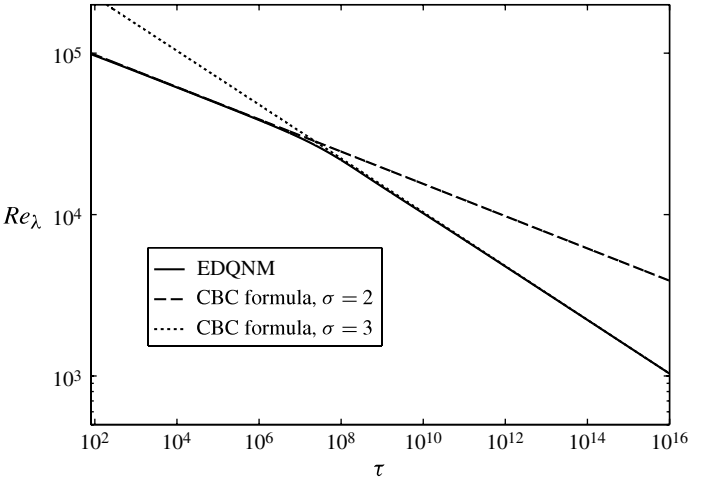

FIGURE 12. Time evolution of the Re_λ number for a composite three-range initial energy spectrum. The case of $\sigma_1 = 3$ and $\sigma_2 = 2$ is investigated.

As a consequence, this case corresponds to the transition from a non-self-similar regime (the spectrum is defined by two independent length scales) to a self-similar regime (obtained once the spectrum has become a classical two-range spectrum).

A similar trend is found for the power-law coefficients related to the analysed physical quantities, as shown in figure 13. The results dealing with the power-law exponents, which are reported in figure 13(*a–c*), are in excellent agreement with the theoretical analysis. The transition between the two regimes is mainly smooth, even if a kink is locally observed before the regime governed by σ_1 is fully established. It appears that this phenomenon is more significant in the prediction of the power-law coefficient related to the characteristic length l_2. Moreover, it seems that the transition between the two states takes a long time to fade, approximately four time decades, and in particular, it appears that the length scale l_2 dynamics are affected by the transition significantly before than those related to the dissipation rate ε. We can also observe that the transition seems to occur slightly earlier than the predicted critical time: this is probably due to the non-negligible effects of the initial transient. Nevertheless, the critical time recovered by (4.20) is a very good estimation of the transition time between the two regimes.

The invariant based on the turbulent kinetic energy u^2 and the characteristic length scale l_2 is shown in figure 13(*d*). The results are again consistent with the theoretical formulation and significant long time invariance is observed. The reader should observe that, as predicted by the theoretical analysis, the invariant based on σ_2 is constant until $l_2 \approx l_1$. It then decays in time, while the invariant based on σ_1 grows until the two scales are of the same order of magnitude. It then becomes an invariant in the latter stages of the numerical simulation.

The computed long-range velocity correlations, which are reported in figure 14, show that during the early stages of the decay $u^2 f \propto r^{-(\sigma_2+1)}$. Conversely, if the energy spectrum is sampled after the critical time t_c, the spatial decay of long-range interactions is governed by the power-law exponent $m = \sigma_1 + 1$.

An interesting result is that during the first evolution time, the spectrum is defined by two independent length scales, and therefore the solution is not self-similar. But the

https://doi.org/10.1017/jfm.2012.396 Published online by Cambridge University Press

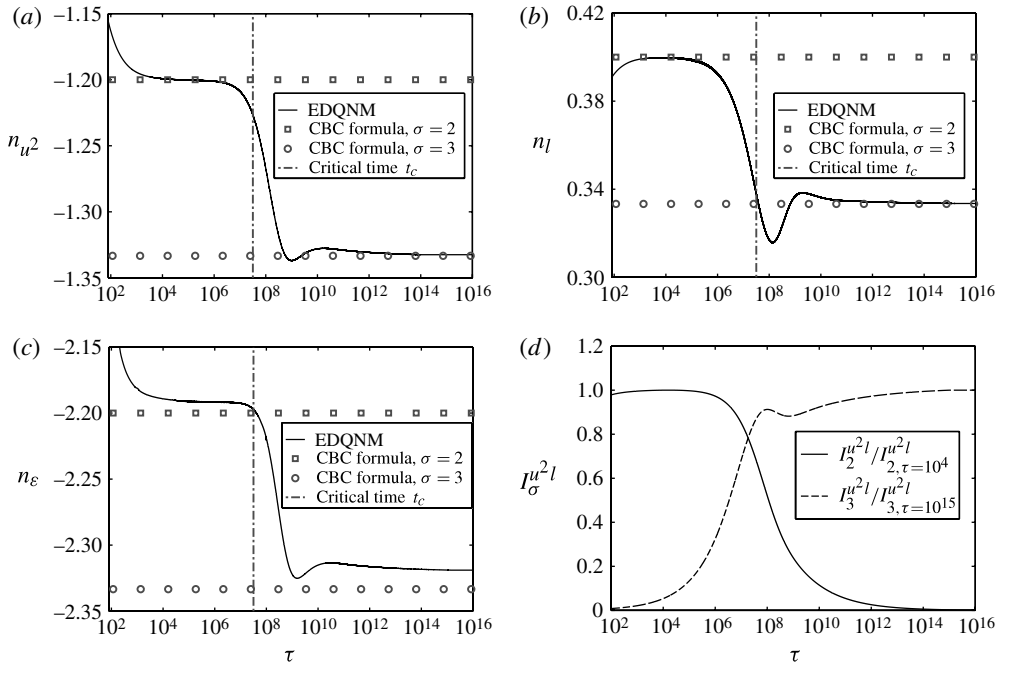

FIGURE 13. Time evolution of power-law exponents relative to (*a*) turbulent kinetic energy, (*b*) characteristic length and (*c*) dissipation rate. (*d*) The invariant based on turbulent kinetic energy and characteristic length scale. A composite three-range energy spectrum is initially imposed at $Re_\lambda = 10^5$ for $\sigma_1 = 3$ and $\sigma_2 = 2$. Symbols denote theoretical values obtained via the CBC-like analysis.

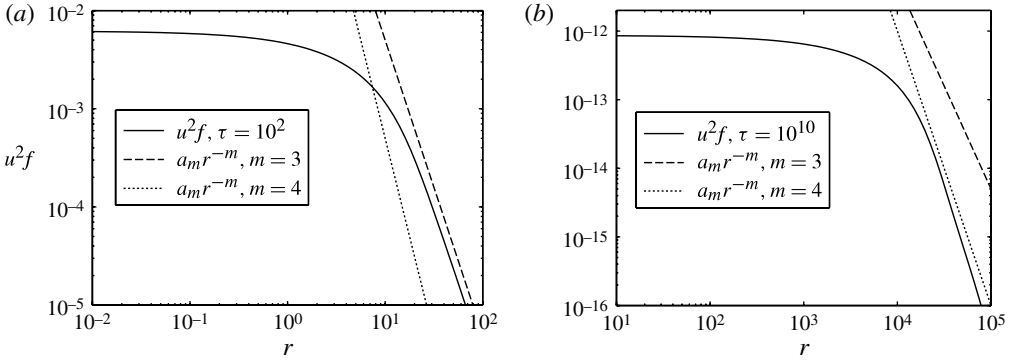

FIGURE 14. Long-range velocity correlations $u^2 f$ obtained by EDQNM simulations. The initial energy spectrum is a three-range spectrum with $\sigma_1 = 3, \sigma_2 = 2$. The energy spectrum was sampled at (*a*) $\tau = 10^2$ and (*b*) $\tau = 10^{10}$; r is expressed in the initial length scale $l_2(0)$ units.

decay is almost identical to a self-similar regime for a classical two-range spectrum with slope σ_2 at very large scales. It may be considered as a pseudo-self-similar regime, from the dynamical point of view. This result is confirmed by the analysis of the nonlinear transfer of energy $T(k)$, which is shown in figure 15 for two different

https://doi.org/10.1017/jfm.2012.396 Published online by Cambridge University Press

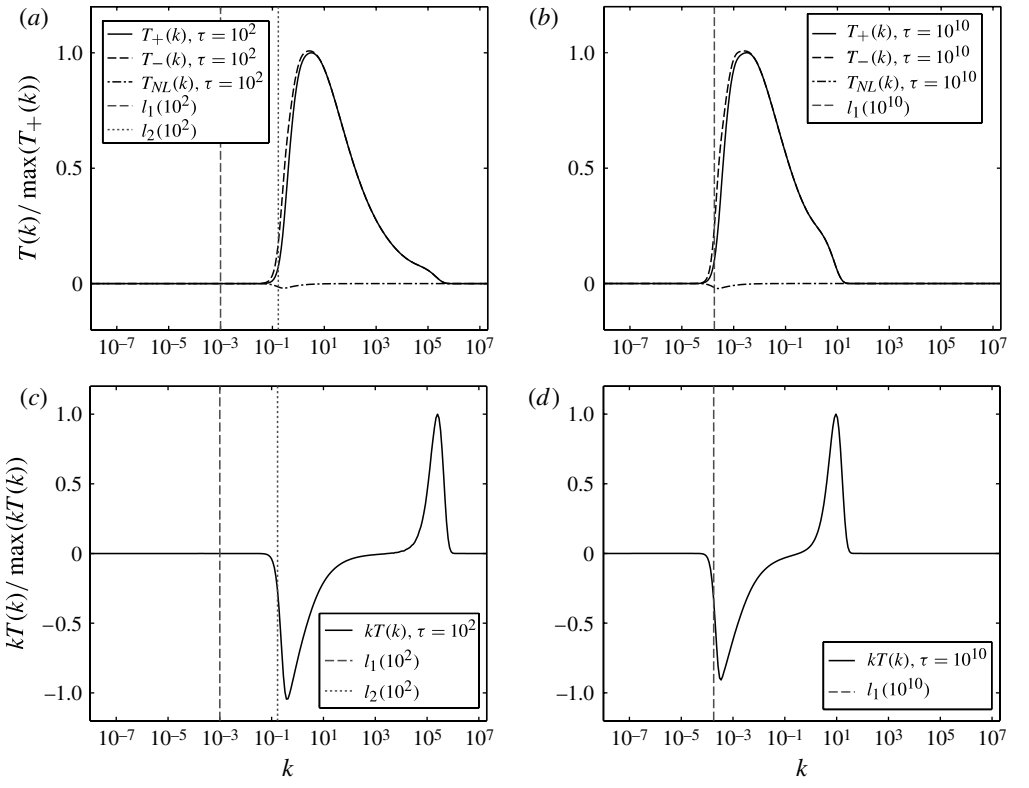

FIGURE 15. (*a,b*) Energy transfer terms $T_+(k)$ (forward cascade), $T_-(k)$ (inverse cascade), $T_{NL}(k)$ (non-local energy transfer). (*c,d*) Premultiplied nonlinear energy transfer $kT(k)$, with $T(k) = T_+(k) - T_-(k) + T_{NL}(k)$. The initial energy spectrum is a three-range spectrum with $\sigma_1 = 3, \sigma_2 = 2$. The energy spectrum was sampled at (*a,c*) $\tau = 10^2 < t_c$ and (*b,d*) $\tau = 10^{10} > t_c$.

simulation times, before and after the bifurcation to a true self-similar state. In both cases, it appears that the scales larger than 10 times the integral scale do not receive or transfer a significant amount of energy; the largest scales can be considered as frozen from the dynamical point of view. Therefore, it appears that the decay regime is governed by the large scales located near the energy spectrum peak and the features of $E(k)$ for $k \simeq 1/l_2$, not by the asymptotically case $k \to 0$. A connection between asymptotic behaviour of the energy spectrum at very large scales and the decay regime is therefore relevant only in the case in which a single range with constant slope exists between $k = 0$ and $k \simeq 1/l$.

5.2. *Three-range energy spectra when the PLE hypothesis does not hold: finite critical time*

Let us now consider the case of a composite three-range energy spectrum for which $3.2 < \sigma_2 \leqslant 4$. From the considerations expressed in the previous section, we expect breakdown of self-similarity if $\sigma_1 - p_1 < \sigma_2 < \sigma_1$, while the system evolves through a pseudo-self-similar and a true self-similar regime if $\sigma_2 < \sigma_1 - p_1$ or $\sigma_2 > \sigma_1$. These two conditions correspond to an infinite and finite critical time, respectively.

https://doi.org/10.1017/jfm.2012.396 Published online by Cambridge University Press

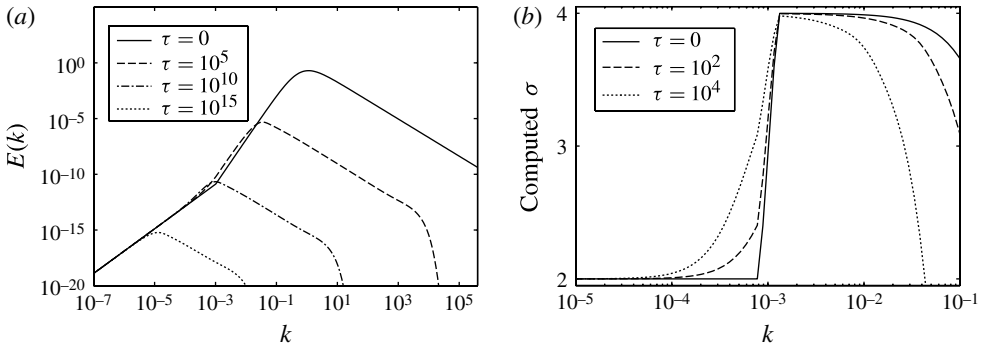

FIGURE 16. (*a*) Time-evolving energy spectra and (*b*) corresponding slope for a composite three-range initial energy spectrum. The case of $\sigma_1 = 2$ and $\sigma_2 = 4$ is investigated.

We consider the case of a finite critical time, choosing the initial conditions $\sigma_1 = 2$ and $\sigma_2 = 4$. The energy spectrum evolution and the corresponding slope are displayed in figure 16. As can be observed in figure 16(*b*), the slope of the energy spectrum evolves in time, since both scales l_1 and l_2 are time-dependent. Nevertheless, since l_2 grows faster than l_1, the two scales will have the same magnitude at the critical time t_c. The use of (4.20) allows us to estimate this time, which for these specific initial conditions is $t_c \approx 10^{13} t_0$. The power-law coefficients related to the turbulent kinetic energy and the other physical quantities investigated are displayed in figure 17(*a–c*). The results confirm the trend that was previously observed in § 5.1. The transition to the true self-similar state is triggered at significantly higher values of the normalized time τ. This delay is due to the lower magnitude of the coefficient n_{l_2} for $\sigma_2 = 4$ compared to the case analysed in the previous section. Moreover, when the simulation time reaches the computed critical time t_c, the transient between the two regimes has faded. These results differ from those found in the case of $\sigma_1 = 3$ and $\sigma_2 = 2$. This is explained by the fact that, because l_1 evolves in time, the part of the energy spectrum located between the two scales tends to exhibit intermediate values of the slope, favouring an earlier transition. This result is confirmed by the slope of the energy spectra shown in figure 16(*b*). The long-range velocity correlations found, which are reported in figure 18, also show very good agreement with the theoretical framework proposed. As a last point, we consider the nonlinear energy transfer $T(k)$, which is shown in figure 19. The reader can observe that the results are very similar to those found in the case $\sigma_1 = 3$ and $\sigma_2 = 2$, yielding the same conclusion about the role of very large scales in the control of the energy decay rate.

5.3. *Three-range energy spectra when the PLE hypothesis does not hold: infinite critical time*

We now address the case of an infinite critical time t_c. This is the case corresponding to breakdown of self-similarity, as two different scales exist at all times. To observe this regime, we impose as initial condition $\sigma_1 = 4$ and $\sigma_2 = 3.7$, which satisfies the requirement $\sigma_1 - p_1 < \sigma_2 < \sigma_1$.

The energy spectrum evolution and the corresponding slope are plotted in figure 20. As observed in figure 20(*b*), the slope of the energy spectrum evolves in time. In particular, it appears that the energy spectrum between the two evolving scales gradually assumes an intermediate slope between the two imposed initial values,

https://doi.org/10.1017/jfm.2012.396 Published online by Cambridge University Press

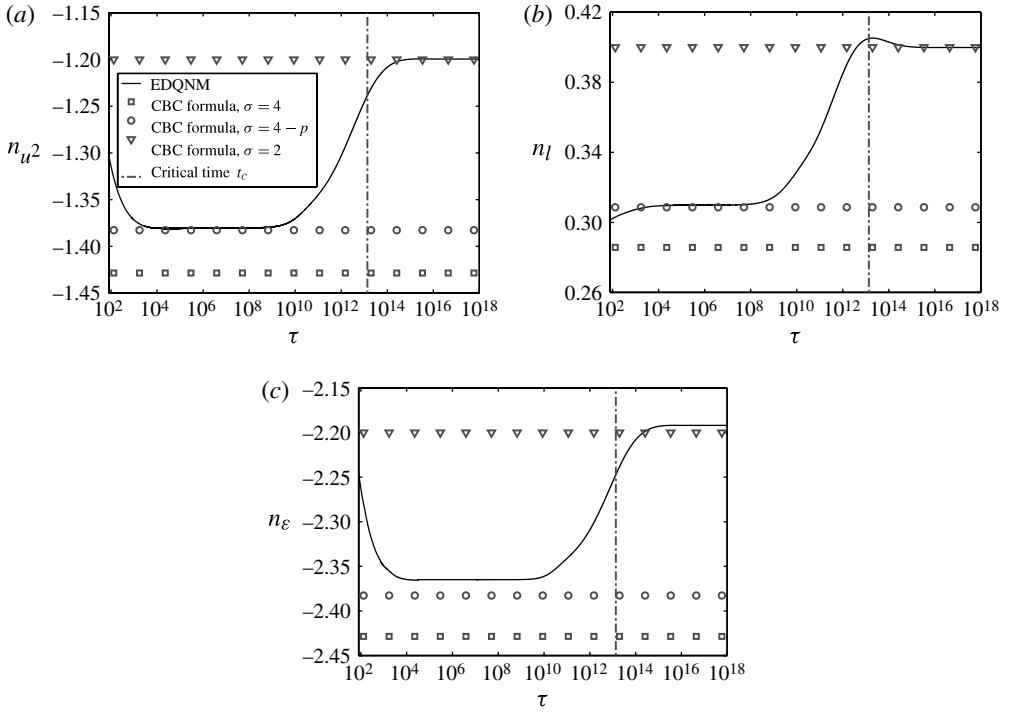

FIGURE 17. Time evolution of the power-law coefficient related to the turbulent kinetic energy in the case of a composite three-range energy spectrum: (*a*) the turbulent kinetic energy, (*b*) the characteristic length scale, and (*c*) the dissipation rate. The case of $\sigma_1 = 2$ and $\sigma_2 = 4$ is investigated.

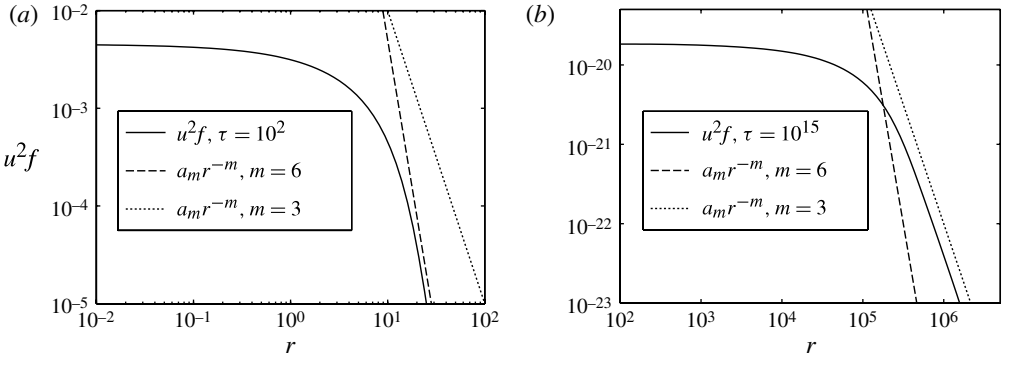

FIGURE 18. Long-range velocity correlations $u^2 f$ obtained by EDQNM simulations. The initial energy spectrum is a three-range spectrum with $\sigma_1 = 2, \sigma_2 = 4$. The energy spectrum was sampled at (*a*) $\tau = 10^2$ and (*b*) $\tau = 10^{15}$; r is expressed in the initial length scale $l_2(0)$ units.

as in the previous case with finite t_c. But now, since the scales diverge, we do not expect that the regime will asymptotically converge to the theoretical regime associated with σ_1.

https://doi.org/10.1017/jfm.2012.396 Published online by Cambridge University Press

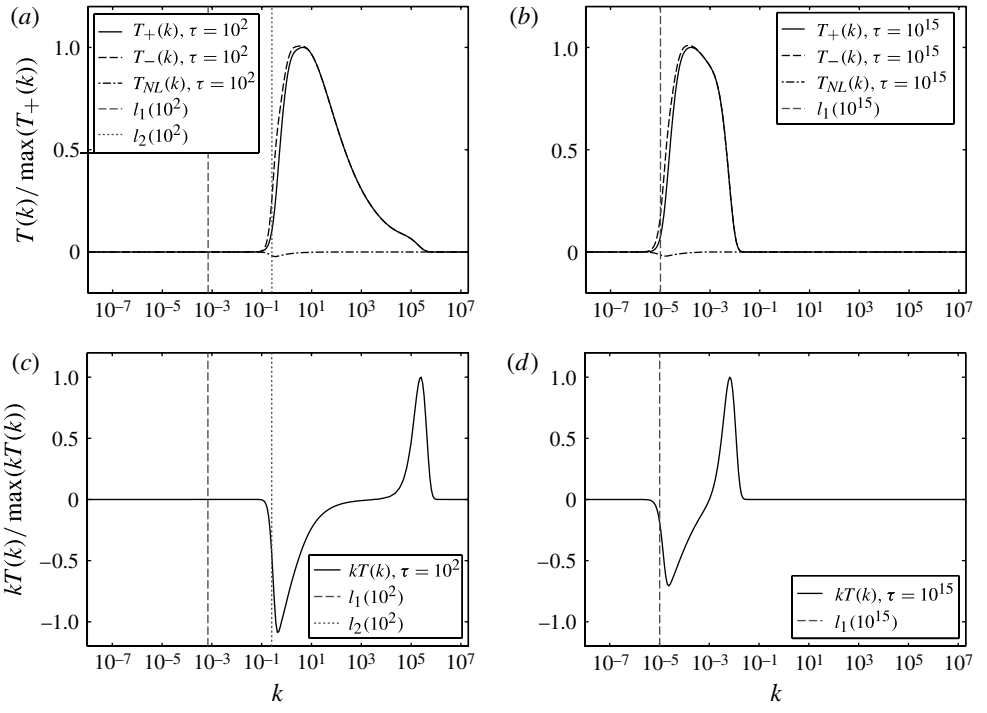

FIGURE 19. (*a,b*) Energy transfer terms $T_+(k)$ (forward cascade), $T_-(k)$ (inverse cascade), $T_{NL}(k)$ (non-local energy transfer). (*c,d*) Premultiplied nonlinear energy transfer $kT(k)$, with $T(k) = T_+(k) - T_-(k) + T_{NL}(k)$. The initial energy spectrum is a three-range spectrum with $\sigma_1 = 2, \sigma_2 = 4$. The energy spectrum was sampled at (*a,c*) $\tau = 10^2 < t_c$ and (*b,d*) $\tau = 10^{15} > t_c$.

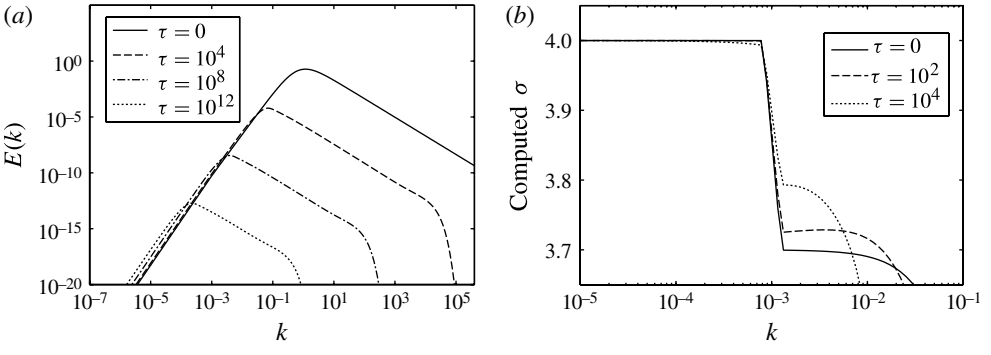

FIGURE 20. (*a*) Time-evolving energy spectra and (*b*) corresponding slope for a composite three-range initial energy spectrum. The case of $\sigma_1 = 4$ and $\sigma_2 = 3.7$ is investigated.

The results shown in figure 21 confirm that the predicted power-law coefficients, after a transient time, are close to the theoretical value associated with the regime $\sigma_2 = 3.7$. Nevertheless, the predicted power-law coefficients evolve in time to a value which is between the regimes associated with $\sigma_2 = 3.7$ and $\sigma_1 = 4$. In this case the turbulent decay, even if not self-similar, can be roughly approximated as being

https://doi.org/10.1017/jfm.2012.396 Published online by Cambridge University Press

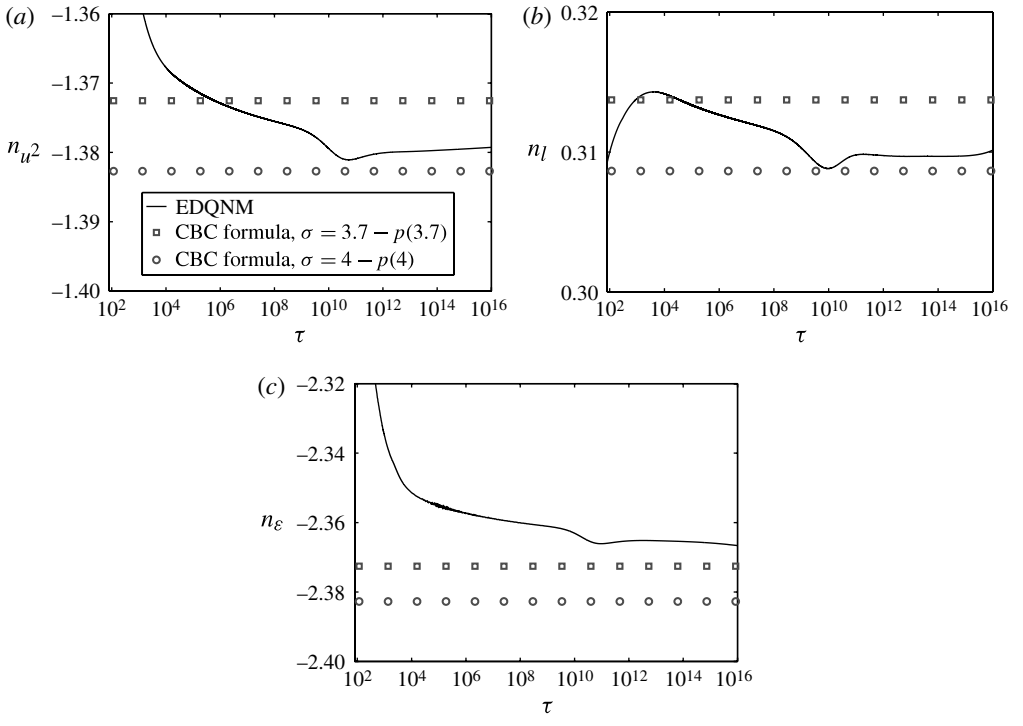

FIGURE 21. Time evolution of the power-law coefficient related to the turbulent kinetic energy in the case of a composite three-range energy spectrum: (*a*) the turbulent kinetic energy, (*b*) the characteristic length scale, and (*c*) the dissipation rate. The case of $\sigma_1 = 4$ and $\sigma_2 = 3.7$ is investigated.

self-similar, and governed by a parameter σ_∞ which is estimated to be in the range $\sigma_2 < \sigma_\infty < \sigma_1$. This conclusion is confirmed by looking at the long-range velocity correlations in figure 22. In fact, the reader can observe that the associated power-law coefficient m is included in the range $5 < m < 6$.

The nonlinear energy transfer term is illustrated in figure 23. As in previous cases, we can observe that energy transfer at very large scales is negligible, supporting the conclusion that the decay regime is not governed by the asymptotic behaviour of the spectrum $E(k \to +\infty)$, but by the features of $E(k)$ at scales close to the peak of the energy spectrum.

6. Conclusions

A theoretical approach to estimating the conditions leading to self-similarity breakdown in HIT decay at high Re_λ number has been proposed and assessed via extended EDQNM simulations.

The classical cases of a two-range energy spectrum for $\sigma = 1, 2, 3, 4$ were first investigated. Excellent agreement between theoretical and numerical results is obtained when the PLE hypothesis is satisfied. The results are in agreement when the power-law coefficients of the physical quantities investigated are considered, as well as when the invariants based on those physical quantities are investigated. The same trend is observed when long-range velocity correlations are analysed.

https://doi.org/10.1017/jfm.2012.396 Published online by Cambridge University Press

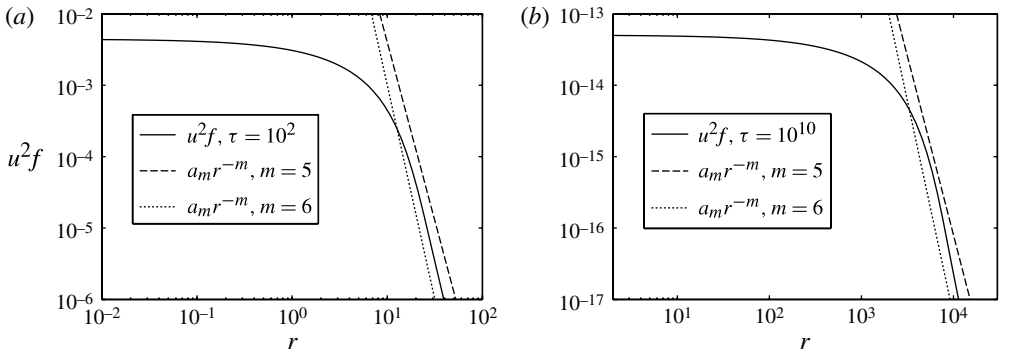

FIGURE 22. Long-range velocity correlations u^2f obtained by EDQNM simulations. The initial energy spectrum is a three-range spectrum with $\sigma_1 = 4$, $\sigma_2 = 3.7$. The energy spectrum was sampled at (*a*) $\tau = 10^2$ and (*b*) $\tau = 10^{10}$; r is expressed in the initial length scale $l_2(0)$ units.

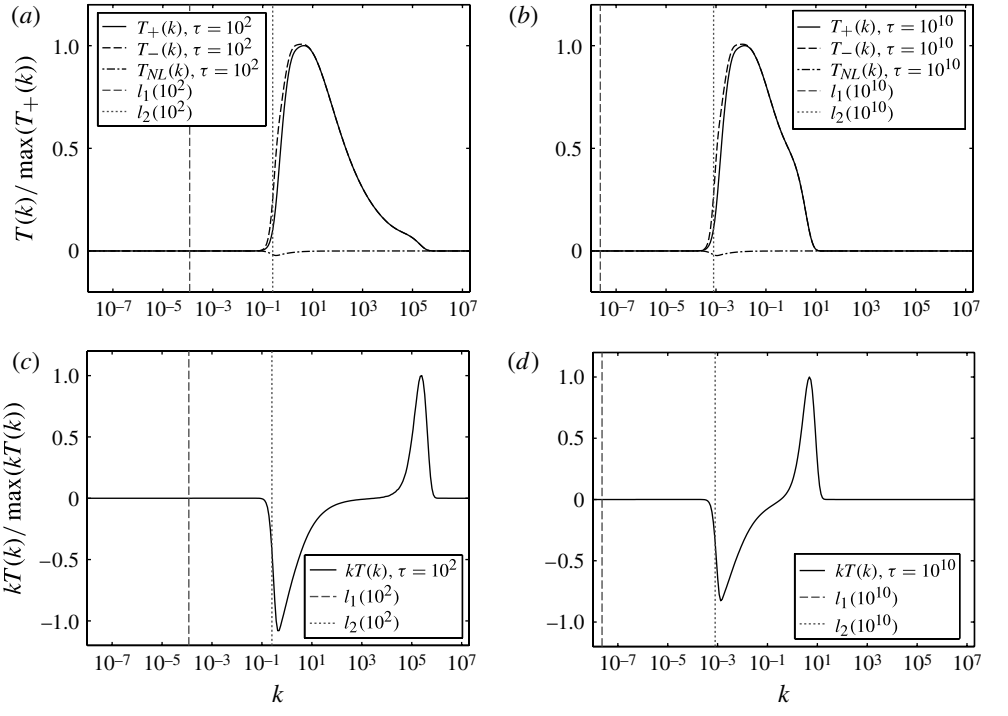

FIGURE 23. (*a,b*) Energy transfer terms $T_+(k)$ (forward cascade), $T_-(k)$ (inverse cascade), $T_{NL}(k)$ (non-local energy transfer). (*c,d*) Premultiplied nonlinear energy transfer $kT(k)$, with $T(k) = T_+(k) - T_-(k) + T_{NL}(k)$. The initial energy spectrum is a three-range spectrum with $\sigma_1 = 4$, $\sigma_2 = 3.7$. The energy spectrum was sampled at (*a,c*) $\tau = 10^2$ and (*b,d*) $\tau = 10^{10}$.

The results of the analysis indicate that, when very high values of the σ parameter are considered, distant triads have a significant impact, leading to failure of the PLE hypothesis, and the classical relation between the decay exponent and the energy

https://doi.org/10.1017/jfm.2012.396 Published online by Cambridge University Press

spectrum slope must be corrected. The present results indicate that the threshold value is about $\sigma = 3.2$.

The decay regime streaming from an initial composite three-range energy spectrum has been successively investigated. If the value of the initial parameters σ_1 and σ_2 is chosen such that for one of the two parameters the relation $\sigma_i \leqslant 3.2$ is true, two different regimes are observed in long time evolution. In the first regime, the spectrum is governed by two independent length scales, resulting in breakdown of self-similarity. However, the dynamics is almost identical to self-similar evolution of a classical two-range spectrum, whose large-scale shape is equal to the energetic large scales in the composite solution. Therefore this regime can be considered as a pseudo-self-similar regime. The second regime is classical self-similar decay. The transition occurs at a critical time $t_c = t_c(\sigma_1, \sigma_2, l_1(0)/l_2(0))$. In the case $\sigma_i > 3.2$, a non-self-similar regime is triggered. The permanence in time of this non-self-similar regime depends on the parameter σ_1 and σ_2 initially imposed, and it cannot be detected solely by analysis of the time evolution of the global physical quantities. In fact, the decay regime will behave as if it were self-similar and driven by the parameter σ_2.

A striking conclusion of the present work is that the decay rate of kinetic energy is not tied to the asymptotic behaviour of large scales, i.e. $E(k \to 0)$ in the general case of a three-range initial energy spectrum. Both theoretical analysis and detailed investigation of nonlinear transfers via EDQNM show that very large scales are not active, in the sense that their associated transfers are almost negligible. On the contrary, large scales close to the peak of the energy spectrum are of major importance in the energy cascade. Therefore, the classical asymptotic results that connect the spectrum slope σ with $E(k) \propto k^{\sigma}$ or the decay rate m of two-point velocity correlation, i.e. $f(r) \propto r^{-m}$, are valid if and only if the spectrum exhibits a single range between $k = 0$ and the spectrum peak.

From the physical point of view, the dependence on detailed features of the spectrum at large scales certainly warrants further investigation, and may at least partially explain the discrepancies observed between experimental data and theoretical predictions, since detailed features of the energy peak may be intimately related to the turbulence production mechanisms, which are not universal.

Appendix. Mathematical details of the EDQNM approximation

EDQNM is a quasi-normal closure used to predict triadic energy transfer. This method has been extensively used to investigate HIT decay, and its relevance is verified by several works reported in the literature (Frisch, Lesieur & Schertzer 1980; Cambon, Mansour & Godeferd 1997). Let us consider the spectral formulation of the Navier–Stokes equation in the form $NS(k)$:

$$\frac{\partial u(k)}{\partial t} = u\,u - \nu k^2 u(k) \tag{A 1}$$

where u is the velocity field and k is a general spectral element. The two-point velocity correlation dynamics can be estimated considering the pair $[k, p]$. If the equations $u(p)\,NS(k)$ and $u(k)\,NS(p)$ are summed and averaged, we obtain

$$\left[\frac{\partial}{\partial t} + \nu(k^2 + p^2)\right] \langle u(k)\,u(p)\rangle = \langle uuu\rangle. \tag{A 2}$$

The equation, which is governed by the third-order moment term on the right-hand side, is equivalent to the Lin equation, which is the spectral counterpart of the

https://doi.org/10.1017/jfm.2012.396 Published online by Cambridge University Press

von Kármán–Howarth equation:

$$\frac{\partial E(k,t)}{\partial t} + 2\nu k^2 E(k,t) = T(k,t), \tag{A 3}$$

where the terms $E(k,t)$ and $T(k,t)$ are the energy spectrum and the spectral energy transfer respectively. A comparison of (A 2) and (A 3) shows that the third-order moments, which represent the interactions between the triad $[k,p,q]$, are equivalent to the nonlinear transfer term between the energetic scales.

If the procedure used to obtain the equation (A 2) is repeated for the triad $[k,p,q]$, the resulting equation is

$$\left[\frac{\partial}{\partial t} + \nu(k^2+p^2+q^2)\right]\langle u(k)\,u(p)\,u(q)\rangle = \langle uuuu\rangle. \tag{A 4}$$

The standard quasi-normal (QN) approximation model is based on the assumption that the fourth-order moments, represented in the right-hand side of (A 4), are associated with a Gaussian random variable. This means that the difference between the actual fourth-order moment and the Gaussian fourth-order moment, which is usually referred to as a fourth-order cumulant, is set to zero as a closure assumption. In this way, the fourth-order moment can be represented by a sum of products of second-order moments (for details see Lesieur 2008):

$$\left[\frac{\partial}{\partial t} + \nu(k^2+p^2+q^2)\right]\langle u(k)\,u(p)\,u(q)\rangle = \sum\langle uu\rangle\langle uu\rangle. \tag{A 5}$$

If the homogeneity constraint is imposed, (A 3) can be conveniently rewritten as

$$\frac{\partial E(k,t)}{\partial t} + 2\nu k^2 E(k,t) = \int_0^t \mathrm{d}\tau \int_{p+q=k} \left[\mathrm{e}^{-\nu(k^2+p^2+q^2)(t-\tau)}\right] \sum\langle uu\rangle\langle uu\rangle\,\mathrm{d}p. \tag{A 6}$$

Correcting the basic assumption of QN closure, Orszag (1970) observes that the effects of fourth-order cumulants can be taken into account by a linear damping term. The resulting eddy-damped quasi-normal (EDQN) equation is given by

$$\left[\frac{\partial}{\partial t} + \nu(k^2+p^2+q^2) + \mu_{kpq}\right]\langle u(k)\,u(p)\,u(q)\rangle = \sum\langle uu\rangle\langle uu\rangle, \tag{A 7}$$

where the term μ_{kpq} represents the eddy-damping rate of the third-order moments associated with the triad $[k,p,q]$. In isotropic turbulence, a very good approximation of this term is

$$\mu_{kpq} = \mu_k + \mu_p + \mu_q, \quad \mu_k = \left[\int_0^k p^2 E(p,t)\,\mathrm{d}p\right]^{1/2}. \tag{A 8}$$

The corresponding equation representing the time evolution of the energy spectrum becomes

$$\frac{\partial E(k,t)}{\partial t} + 2\nu k^2 E(k,t) = \int_0^t \mathrm{d}\tau \int_{p+q=k} \left[\exp(-(\mu_{kpq} + \nu(k^2+p^2+q^2))(t-\tau))\right] \times \sum\langle uu\rangle\langle uu\rangle\,\mathrm{d}p. \tag{A 9}$$

Nevertheless, the EDQN approximation does not always reproduce a physical energy spectrum, as negative values in the energy magnitude have been observed under

https://doi.org/10.1017/jfm.2012.396 Published online by Cambridge University Press

particular conditions. This drawback can be corrected by a *Markovianization* operation. In the resulting model, the characteristic time $(\mu_{kpq} + \nu(k^2 + p^2 + q^2))^{-1}$ associated with the integrand in the right-hand side of (A 9) is assumed to be negligible with respect to the characteristic evolution time $\sum\langle uu\rangle\langle uu\rangle$. This leads to dramatic simplification of (A 9), since the integral can be approximated by

$$\int_0^t \left[\exp(-(\mu_{kpq} + \nu(k^2 + p^2 + q^2))(t - \tau))\right] \mathrm{d}\tau$$
$$= \frac{1 - \exp(-(\mu_{kpq} + \nu(k^2 + p^2 + q^2))t)}{\mu_{kpq} + \nu(k^2 + p^2 + q^2)} = \Theta_{kpq}. \tag{A 10}$$

The Markovianization procedure leads to the standard version of the EDQNM model, which reads

$$\frac{\partial E(k,t)}{\partial t} + 2\nu k^2 E(k,t) = T_E(k,t) = T_+(k,t) - T_-(k,t)$$
$$= \int_{p+q=k} \Theta_{kpq} \sum\langle uu\rangle\langle uu\rangle(t)\,\mathrm{d}p. \tag{A 11}$$

The EDQNM approach is able to predict accurately the three-point velocity correlations when the elements of the triad $[k, p, q]$ are of the same order of magnitude, because of the logarithmic discretization of wavenumber space. Conversely, very elongated non-local triads are exactly recovered only when the triads $k = p$ or $k = q$ are taken into account. This can have a significant impact on the accuracy of the predicted results, particularly if the two-point velocity correlation decays fast. A possible solution is to correct (A 11), introducing the analytically computed non-local interactions.

Following the work by Lesieur & Schertzer (1978), the EDQNM equation is extended to obtain high accuracy for very elongated non-local triads, by explicitly including the contribution of these triads:

$$\frac{\partial E(k,t)}{\partial t} + 2\nu k^2 E(k,t) = T_E(k,t) + T_{NL}(k,t). \tag{A 12}$$

The non-local energy transfer term $T_{NL}(k,t)$ is

$$T_{NL}(k,t) = -\frac{2}{15}k^2 E(k,t) \int_{k/a}^{+\infty} \Theta_{kpp} \left[5E(p,t) + p\frac{\partial E(p,t)}{\partial p}\right] \mathrm{d}p$$
$$+ \frac{14}{15}k^4 \int_{k/a}^{+\infty} \Theta_{kpp} \frac{E^2(p,t)}{p^2}\,\mathrm{d}p \tag{A 13}$$

where $a = 0.2$. The addition of the non-local energy transfer term improves the accuracy of the results if fast-decaying two-point correlations are considered. Preliminary tests showed that, in the case of Batchelor turbulence, the slope of the energy spectrum is obtained with an error lower than 1 % for all the decay time analysed. Conversely, an error up to 8 % was observed using the standard version of the EDQNM model.

REFERENCES

BATCHELOR, G. K. 1953 *The Theory of Homogeneous Turbulence*. Cambridge University Press.

BOS, W. J. T., SHAO, L. & BERTOGLIO, J. P. 2007 Spectral imbalance and the normalized dissipation rate of turbulence. *Phys. Fluids* **19**, 045101.

https://doi.org/10.1017/jfm.2012.396 Published online by Cambridge University Press

CAMBON, C., MANSOUR, N. N. & GODEFERD, F. S. 1997 Energy transfer in rotating turbulence. *J. Fluid Mech.* **337**, 303–332.

CLARK, T. T. & ZEMACH, C. 1998 Symmetries and the approach to statistical equilibrium in isotropic turbulence. *Phys. Fluids* **10** (11), 2846–2858.

COMTE-BELLOT, G. & CORRSIN, S. 1966 The use of a contraction to improve the isotropy of grid-generated turbulence. *J. Fluid Mech.* **25**, 657–682.

DAVIDSON, P. A. 2004 *Turbulence: An Introduction for Scientists and Engineers*. Oxford University Press.

DAVIDSON, P. A. 2009 The role of angular momentum conservation in homogeneous turbulence. *J. Fluid Mech.* **632**, 329–358.

DAVIDSON, P. A. 2011 The minimum energy decay rate in quasi-isotropic grid turbulence. *Phys. Fluids* **23**, 085108.

EYINK, G. L. & THOMSON, D. J. 2000 Free decay of turbulence and breakdown of self-similarity. *Phys. Fluids* **12** (3), 477–479.

FRENKEL, A. L. 1984 Decay of homogeneous turbulence in three-range models. *Phys. Lett.* A **102** (7), 298–302.

FRENKEL, A. L. & LEVICH, E. 1983 'Statistical helicity invariant' and decay of inertial turbulence. *Phys. Lett.* A **98** (1–2), 25–27.

FRISCH, U., LESIEUR, M. & SCHERTZER, D. 1980 Comments on the quasi-normal Markovian approximation for fully-developed turbulence. *J. Fluid Mech.* **97**, 181–192.

GEORGE, W. K. 1992 The decay of homogeneous isotropic turbulence. *Phys. Fluids* A **4** (7), 1492–1509.

GEORGE, W. K. & WANG, H. 2009 The exponential decay of homogeneous turbulence. *Phys. Fluids* A **21**, 025108.

HINZE, J. O. 1975 *Turbulence*. *McGraw-Hill Series in Mechanical Engineering*, 790 pages.

HUANG, M. J. & LEONARD, A. 1994 Power-law decay of homogeneous turbulence at low Reynolds numbers. *Phys. Fluids* **6**, 3765–3775.

ISHIDA, T., DAVIDSON, P. A. & KANEDA, Y. 2006 On the decay of isotropic turbulence. *J. Fluid Mech.* **564**, 455–475.

KOLMOGOROV, A. N. 1941 On the degeneration of isotropic turbulence in an incompressible viscous fluid. *Dokl. Akad. Nauk SSSR* **31** (6), 538–541.

KROGSTAD, P.-Å. & DAVIDSON, P. A. 2010 Is grid turbulence Saffman turbulence? *J. Fluid Mech.* **642**, 373–394.

KROGSTAD, P.-Å. & DAVIDSON, P. A. 2011 Freely decaying, homogeneous turbulence generated by multi-scale grids. *J. Fluid Mech.* **680**, 417–434.

KROGSTAD, P.-Å. & DAVIDSON, P. A. 2012 Near-field investigation of turbulence produced by multi-scale grids. *Phys. Fluids* **24**, 035103.

LESIEUR, M. & SCHERTZER, D. 1978 Self similar decay of high Reynolds number turbulence. *J. de Mécanique* **17** (4), 609–646.

LESIEUR, M. 2008 *Turbulence in Fluids*, 4th edn. Springer.

LLOR, A. 2011 Langevin equation of big structure dynamics in turbulence: Landau's invariant in the decay of homogeneous isotropic turbulence. *Eur. J. Mech.* B **30**, 480–504.

MANSOUR, N. N. & WRAY, A. A. 1994 Decay of isotropic turbulence at low Reynolds number. *Phys. Fluids* **6**, 808–814.

MAZELLIER, N. & VASSILICOS, J. C. 2010 Turbulence without Richardson-like cascade. *Phys. Fluids* **22**, 075101.

MELDI, M., SAGAUT, P. & LUCOR, D. 2011 A stochastic view of isotropic turbulence decay. *J. Fluid Mech.* **668**, 351–362.

MOHAMED, M. S. & LARUE, J. C. 1990 The decay power law in grid-generated turbulence. *J. Fluid Mech.* **219**, 195–214.

MONIN, A. S. & YAGLOM, A. M. 1975 *Statistical Fluid Mechanics: Mechanics of Turbulence*, vol. 2. MIT Press.

OBERLACK, M. 2002 On the decay exponent of isotropic turbulence. *Proc. Appl. Math. Mech.* **1**, 294–297.

ORSZAG, S. A. 1970 Analytical theories of turbulence. *J. Fluid Mech.* **41**, 363–386.

https://doi.org/10.1017/jfm.2012.396 Published online by Cambridge University Press

POPE, S. B. 2000 *Turbulent Flows*. Cambridge University Press.

RISTORCELLI, J. R. 2003 The self-preserving decay of isotropic turbulence: analytic solutions for energy and dissipation. *Phys. Fluids* **15**, 3248–3250.

RISTORCELLI, J. R. 2006 Passive scalar mixing: analytic study of time scale ratio, variance and mix rate. *Phys. Fluids* **18**, 075101.

RISTORCELLI, J. R. & LIVESCU, D. 2004 Decay of isotropic turbulence: fixed points and solutions for non-constant $G \sim R_\lambda$ palinstrophy. *Phys. Fluids* **16**, 3487–3490.

SAFFMAN, P. J. 1967 The large-scale structure of homogeneous turbulence. *J. Fluid Mech.* **27**, 581–593.

SAGAUT, P. & CAMBON, C. 2008 *Homogeneous Turbulence Dynamics*. Cambridge University Press.

SKRBEK, L. & STALP, S. R. 2000 On the decay of homogeneous isotropic turbulence. *Phys. Fluids* **12**, 1997–2019.

SPEZIALE, C. G. & BERNARD, P. S. 1992 The energy decay in self-preserving isotropic turbulence revisited. *J. Fluid Mech.* **241**, 645–667.

TAYLOR, G. I. 1935 Statistical theory of turbulence. *Proc. R. Soc. Lond.* A **151**, 421–444.

TCHOUFAG, J., SAGAUT, P. & CAMBON, C. 2012 Spectral approach to finite Reynolds number effects on Kolmogorov's 4/5 law in isotropic turbulence. *Phys. Fluids* **24**, 015107.

VASSILICOS, J. C. 2011 An infinity of possible invariants for decaying homogeneous turbulence. *Phys. Lett.* A **375**, 1010–1013.

VALENTE, P. C. & VASSILICOS, J. C. 2012 Dependence of decaying homogeneous isotropic turbulence on inflow conditions. *Phys. Lett.* A **376**, 510–514.

https://doi.org/10.1017/jfm.2012.396 Published online by Cambridge University Press